

Development of a time resolved x-ray diffraction diagnostic for dynamic laser compression experiments at the National Ignition Facility (NIF)

Kalpani Werellapatha,
Postdoctoral research associate
Lawrence Livermore National Lab
On behalf of the time resolved x-ray diffraction team

PI and Campaign RI: Laura Robin Benedetti

LLNL-PRES-837557



Many thanks to all the members of the XRDt team

Laura Robin Benedetti
Nathan Palmer
Martin Gorman
Kalpani Werellapatha

Materials Physics

Dave Braun
Federica Coppari
Jon Eggert
Amy Jenei

Kinetics (&) Theory

Christine Wu
Will Schill
Jon Belof
Philip Myint

Backlighters & Plasma Physics

Gareth Hall
Andy Krygier
Christine Krauland
Elijah Kemp
Marilyn Schneider

Consulting physics

Ray Smith
Ryan Rygg
Rip Collins
Rick Kraus
Suzanne Ali

Electrical Engineering

Peter Nyholm
Emily Hurd
Matt Dayton
Casandra Durand
Brad Golick

Mechanical Design

Brad Petre
Jeremy Huckins
Josh Tabamina

Project Engineering

Camelia Stan
Matt Bruhn
Korbie Le Galloudec

Target Fab and SMEs

Nathan Masters
Bryan Ferguson
Neal Bhandarkar
Chuck Heinbockel
Rick Heredia
Dan Kalantar

Oversight

Dave Bradley
Joe Kilkenny
Warren Hsing
Perry Bell
Arthur Carpenter
Sabrina Nagel
Andy MacKinnon
Jim McNaney

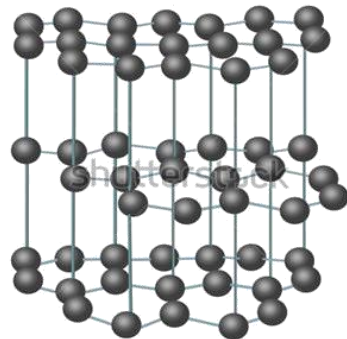


We've developed a test diagnostic that collects multiple frames of time-resolved x-ray diffraction data on hCMOS sensors with laser ramp compression experiments at NIF

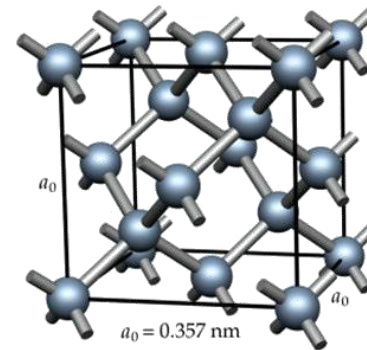
- Two hCMOS sensors with 1-2 ns exposure time can collect 4 frames of data during phase transition of Pb, ramp compressed to 1 Mbar
- We designed and optimized a ~10 ns long Ge backlighter as the x-ray source
- The design and development of this diagnostic will improve future XRDt diagnostics at the National Ignition Facility

Application of high pressure can change material properties fundamentally

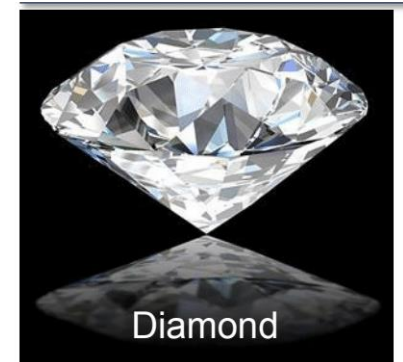
The equation of state and the strength of materials require accurate determination of its atomic structure



graphite



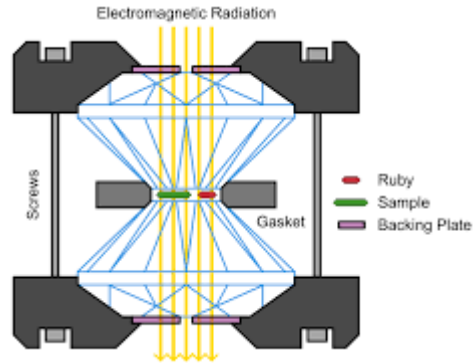
diamond



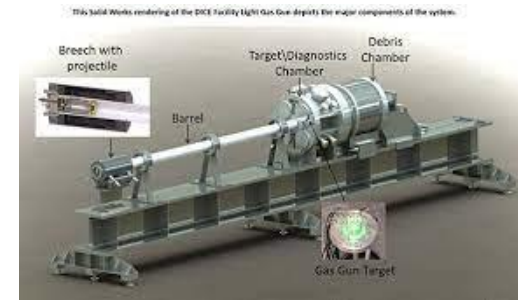
Compared to diamond, graphite has lower density, lower bulk modulus and lower yield strength

The dynamics of material response to pressure loading depends on the strain rate and the peak pressure

DACs

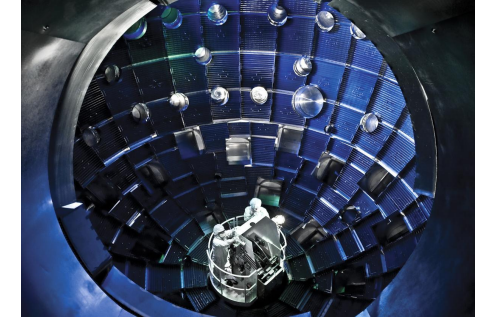


Gas guns

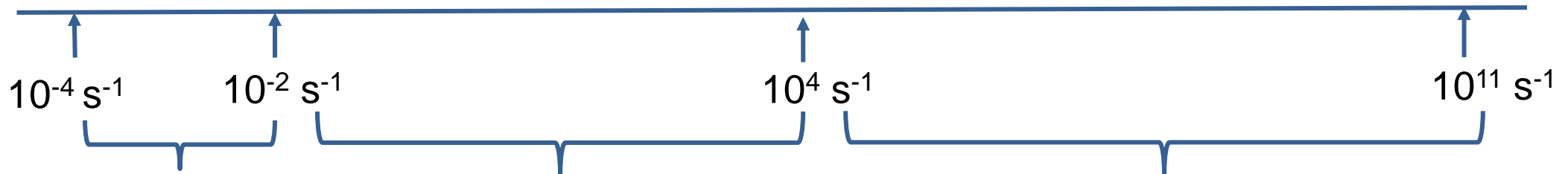


Sandia.gov

Laser facilities



Strain rates

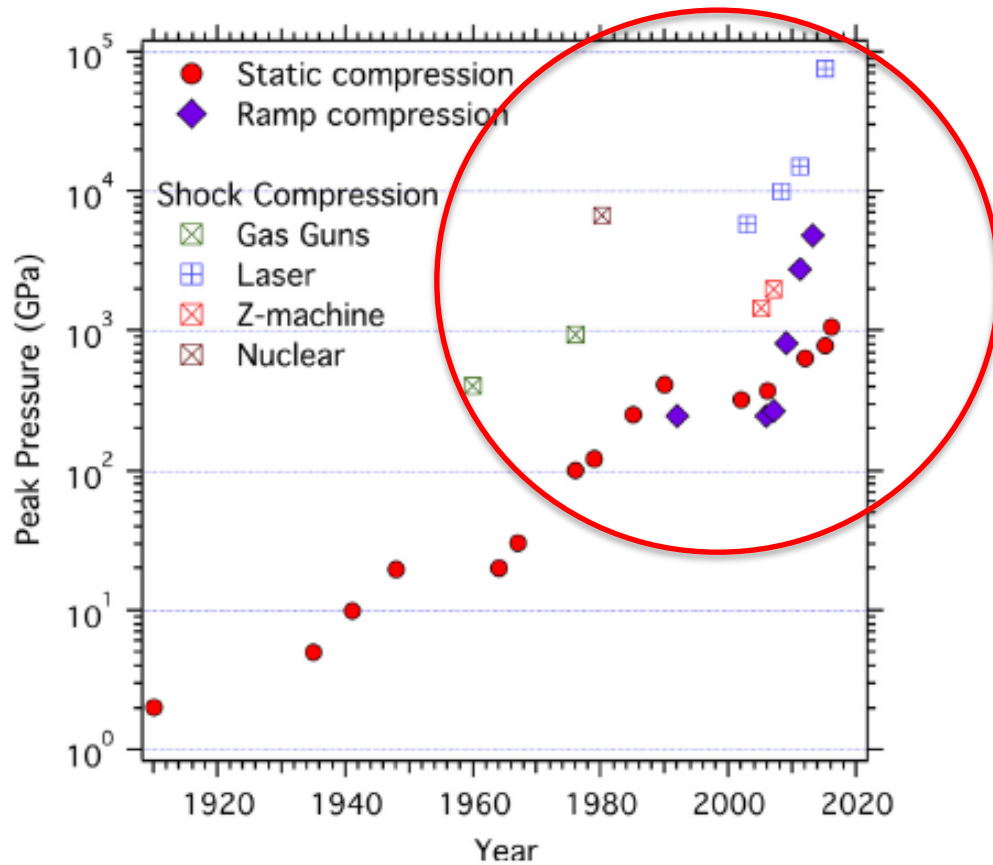


Static pressures
(DACs, large volume presses)

Dynamic diamond anvil cells

Dynamic pressures (ramp and shock compression)
(gas guns, explosives, lasers)

New capabilities in static and dynamic compression have pushed peak pressures up to GPa and TPa regime

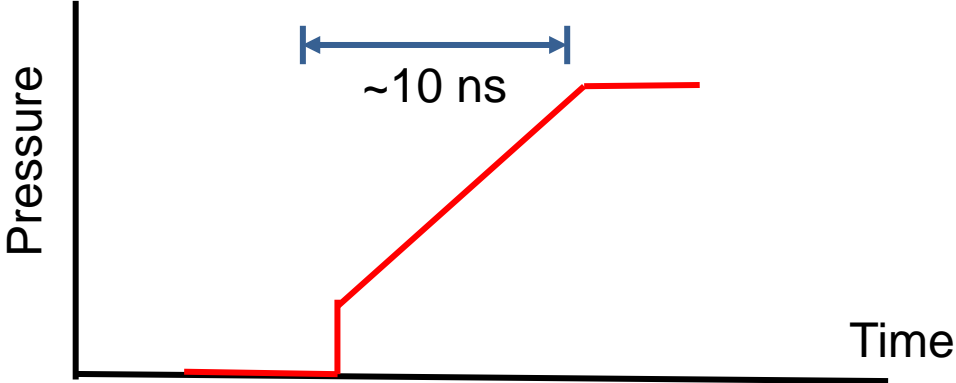


For the development of time-resolved XRD diagnostic to measure phase transition dynamics and kinetics, we're most interested in dynamic laser compression methods

Duffy and Smith, Frontiers in Earth Sciences, 2019.

Time scales of dynamic laser compression experiments can be extended to tens of nanoseconds

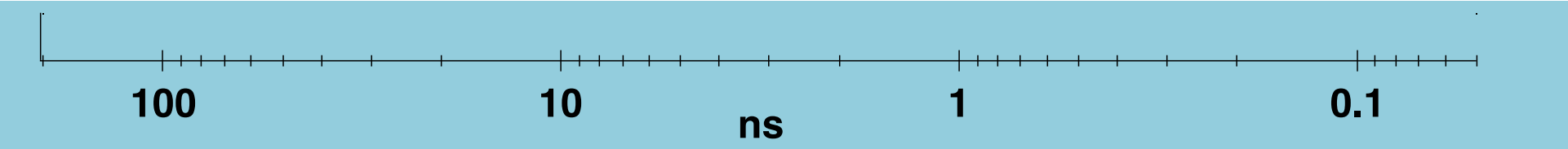
Example:
laser ramp compression



Highly reconstructive or
chemical transformations

Barely overdriven

Over driven phase transitions
can happen this fast at NIF



Dynamic laser compression experiments allow solid state experiments to reach very high pressures and strain rates

2020 ultrahigh-intensity laser facilities



NIF
Max. reported ramp pressure ~5 TPa

OMEGA -60
Max. reported ramp pressure ~1.3 TPa

OMEGA-EP
Max. reported ramp pressure ~1.3 TPa

LUL
Max. reported ramp pressure ~1 TPa

LULI2000
Max. reported ramp pressure ~0.2 TPa

www.laserfocusworld.com

Duffy and Smith, 2019, Frontiers in Science

Large laser facilities provide many advantages for dynamic laser compression studies over synchrotrons and XFELs

At DCS:
100 J
laser



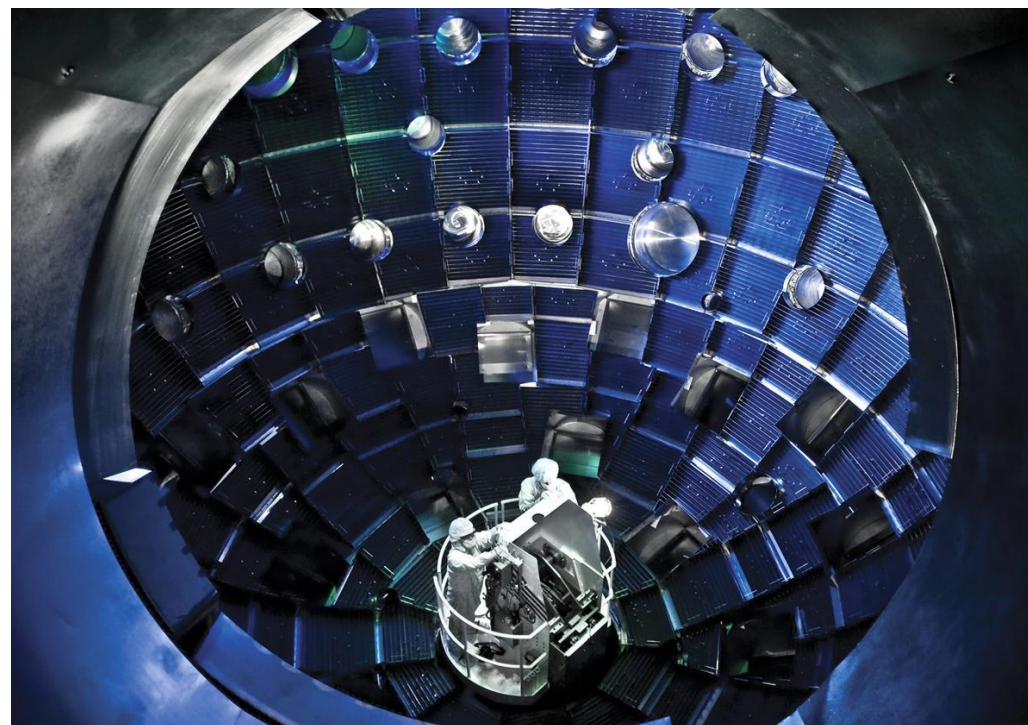
Synchrotrons : (ex. DCS of APS – Argonne)

At LCLS:
50 J
laser



XFELs : (ex. LCLS – Stanford)

Large laser facilities (ex. NIF)

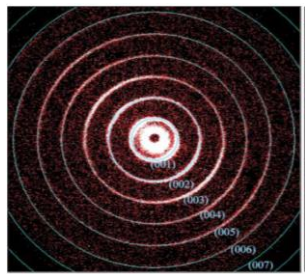
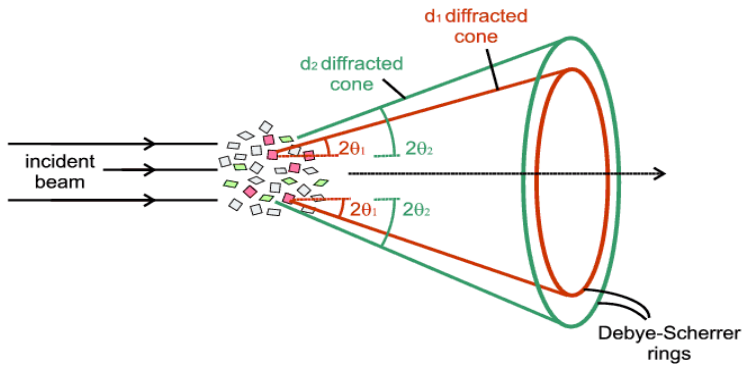


Laser energy:
1.8 MJ

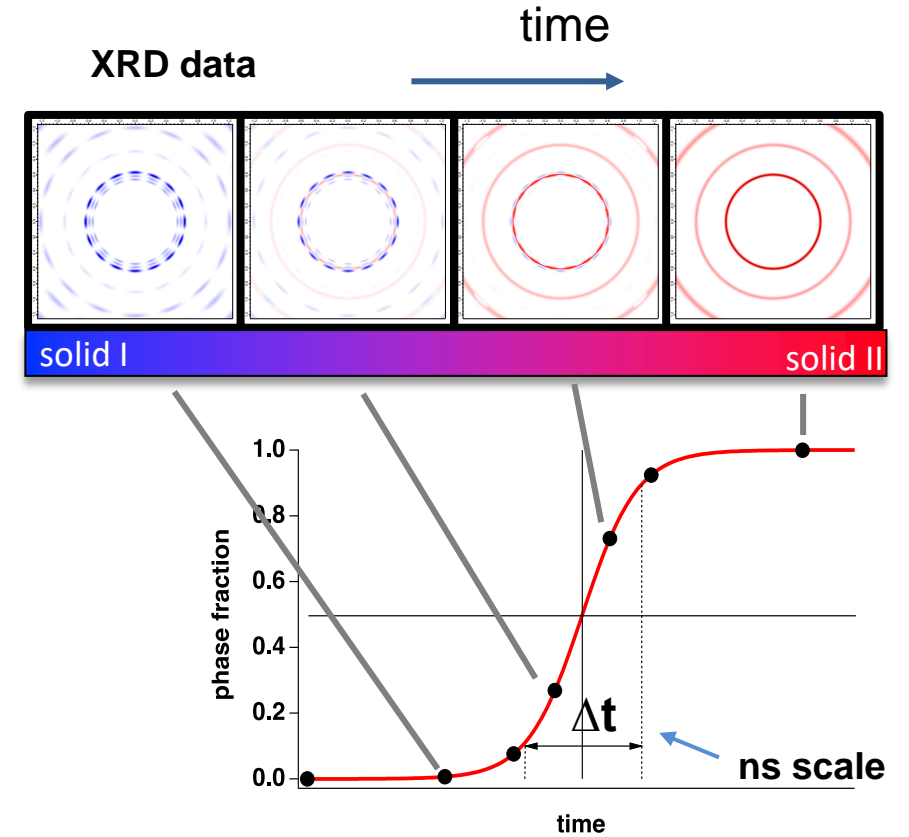
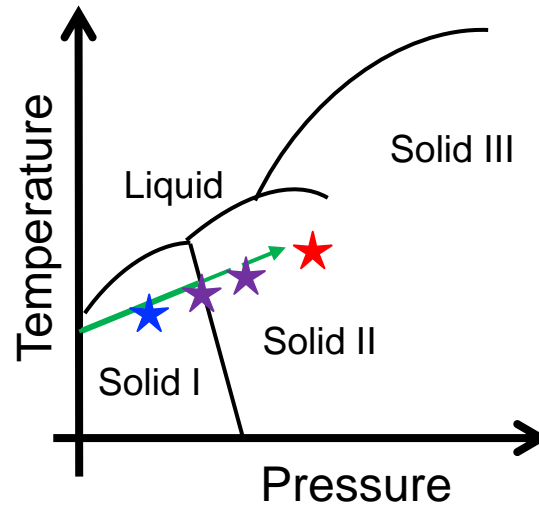
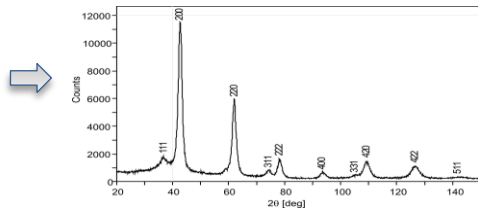
Larger pressures along a precise thermodynamic path
-Advanced beam smoothing techniques
-Advanced pulse shaping capabilities.

We combine dynamic laser compression methods with x-ray diffraction to study phase transition kinetics

X-ray diffraction is measuring the distance between atoms



Debye - Scherrer rings

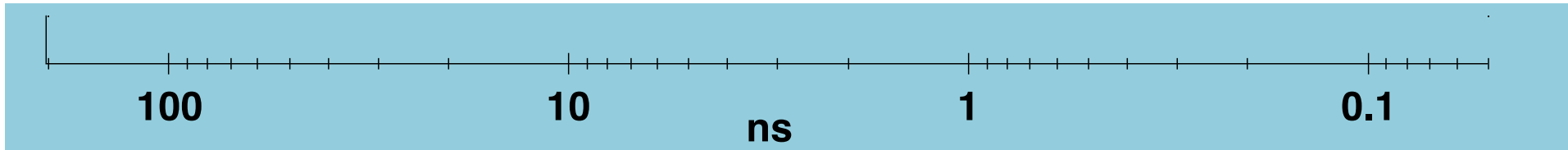


Time scales for phase transitions with laser compression indicate we need really fast detectors with multiple frames of data

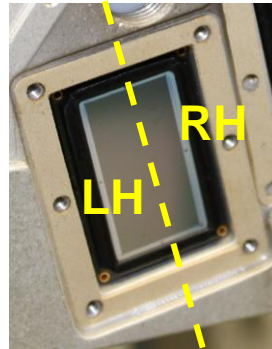
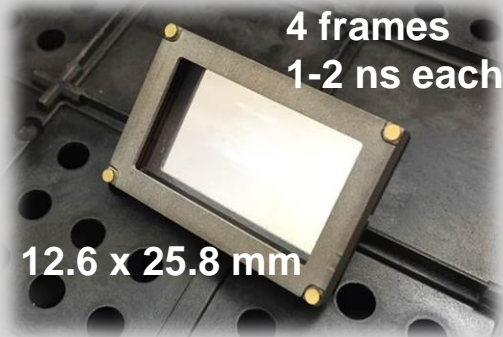
Highly reconstructive or chemical transformations

Barely overdriven

Over driven phase transitions can happen this fast at NIF



- hCMOS multiframe ns x-ray sensor (SNL/LLNL)



Each pixel collects 4 frames of data

Exposure time
1-2 ns

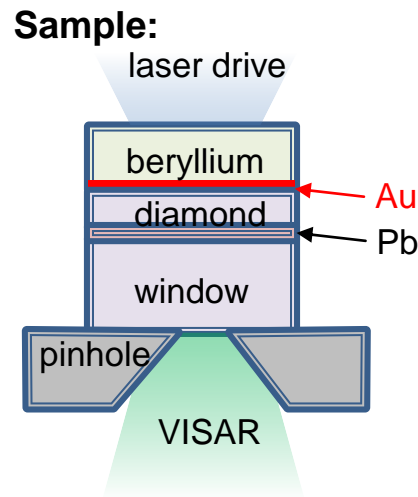
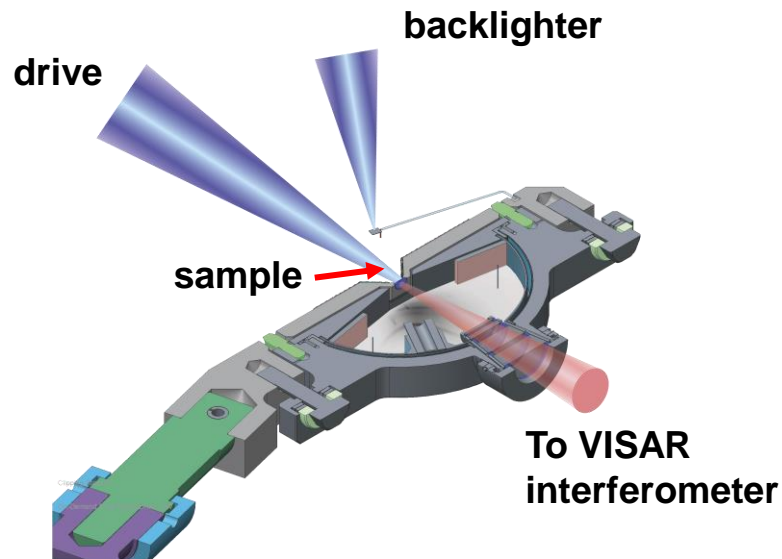
Interframe time
~1 ns

LH and RH can be delayed in time to get continuous coverage

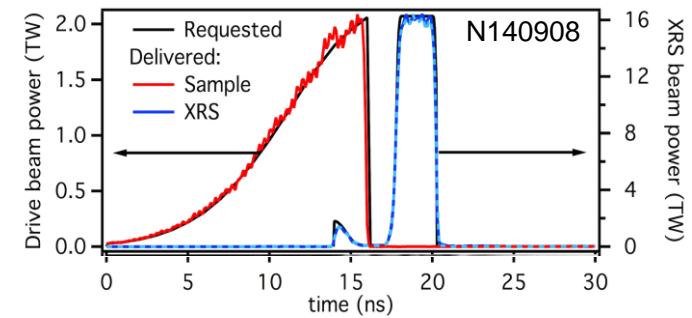
Our design is influenced by the success of TARDIS (Target Diffraction *In Situ*) diagnostic at NIF

TARDIS diagnostic at NIF have observed many new materials at high P, however, it is not designed to observe x-ray diffraction more than two times during phase transitions in one single shot

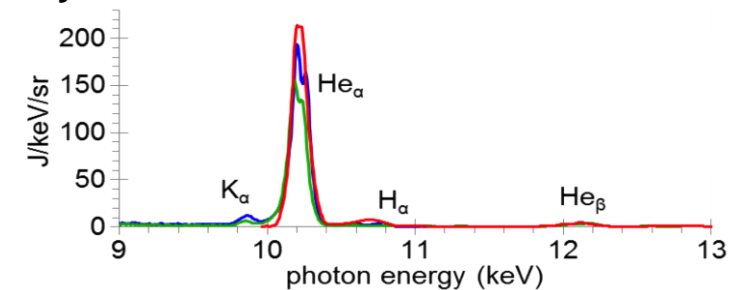
TARDIS – x-ray diffraction to image plates



Laser drive:



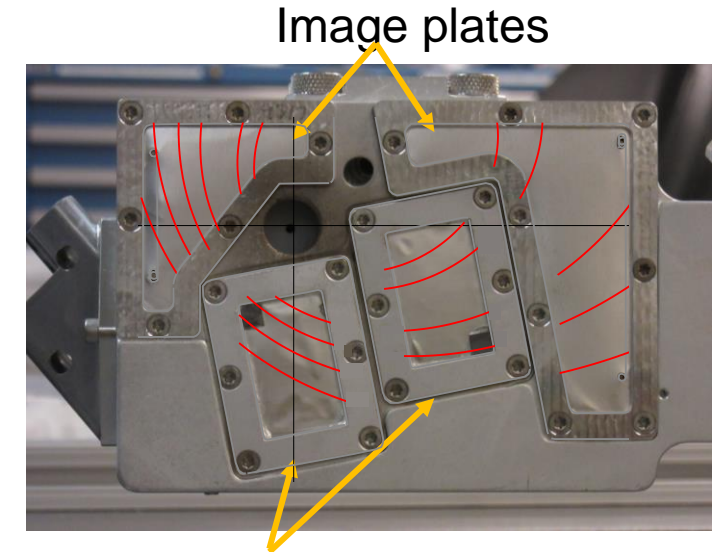
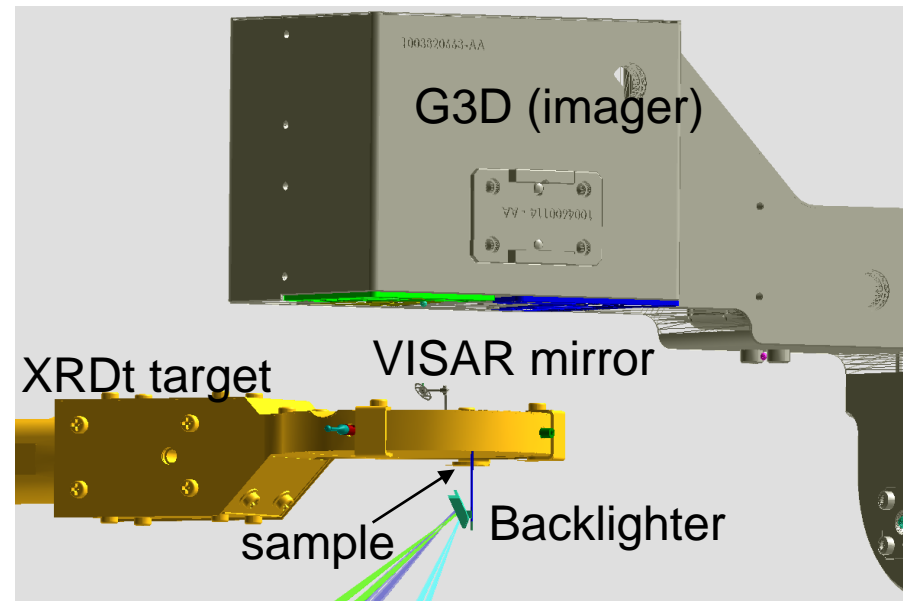
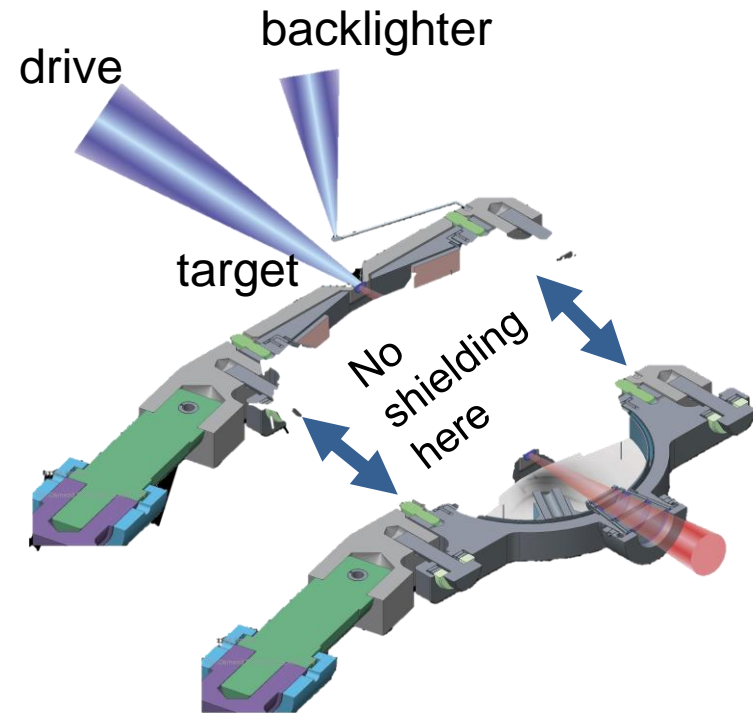
X-ray source:



Rygg, J. R. et al. Powder diffraction from solids in the terapascal regime. Rev. Sci. Instrum. 83, 113904 (2012).
 Rygg, J. R. et al. X-ray diffraction at the National Ignition Facility. Rev. Sci. Instrum. 91,043902 (2020).

Experimental geometry takes advantage of successful implementations of TARDIS diagnostic at NIF

XRDt platform with gated diffraction development(G3D) diagnostic



2 hCMOS sensors embedded

XRDt – x-ray diffraction to hCMOS sensors

Development of the experimental diagnostic requires consideration of various constraints

- **Laser constraints**

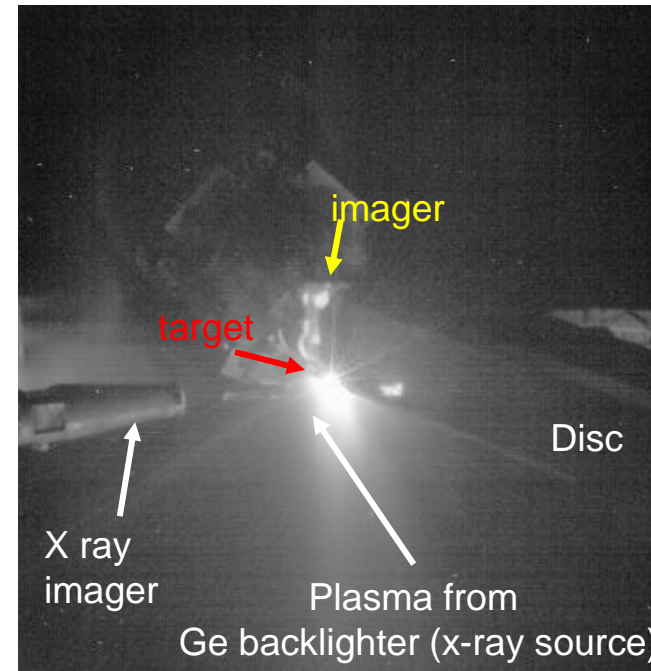
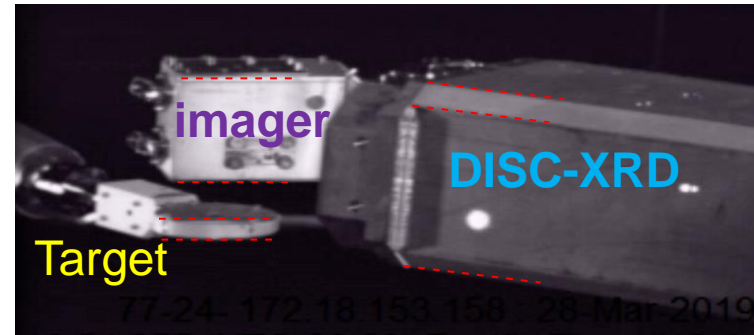
NIF has 192 laser beams with limited range of pointing, focal spot size and pulse shape. Also, residual infrared beams

- **Chamber constraints**

Components cannot come too close to each other because of general alignment constraints. No external x-ray source

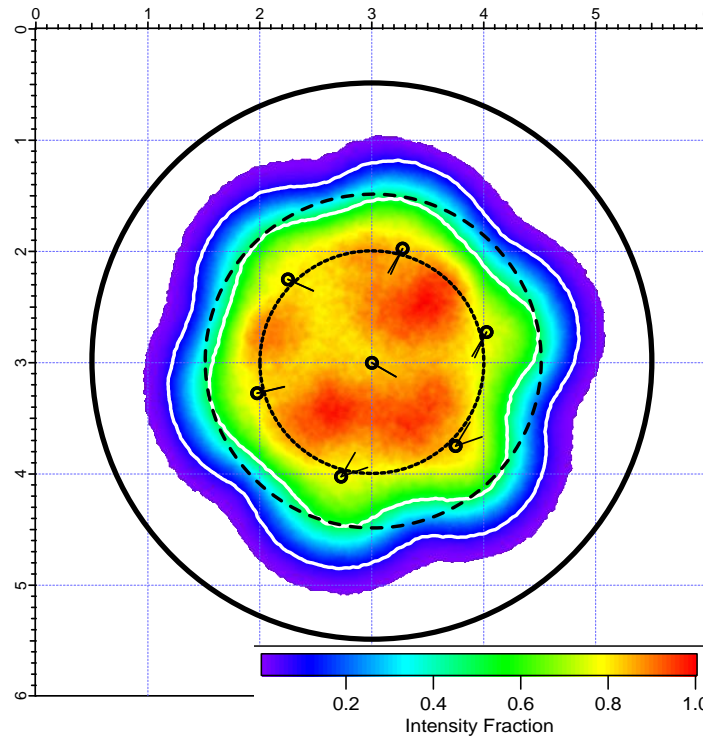
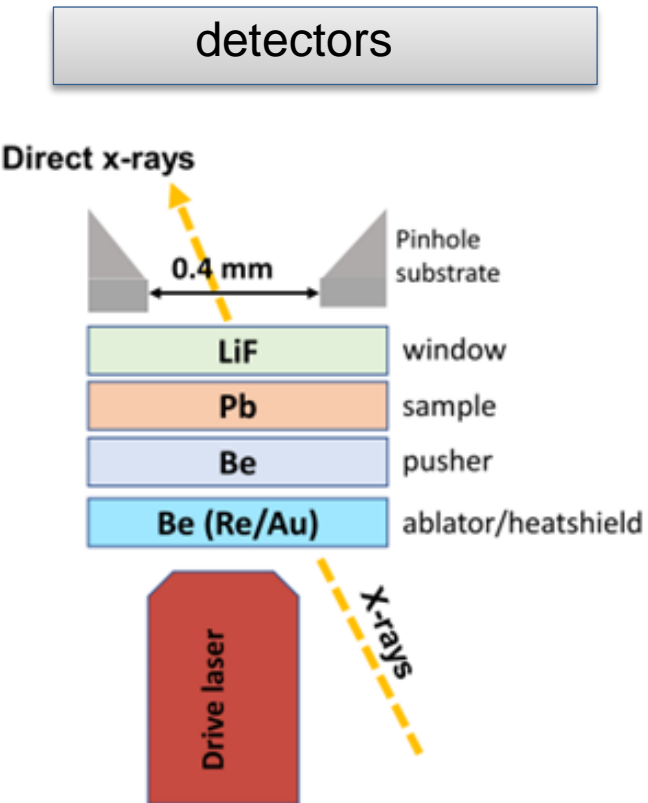
- **Detection constraints**

high vacuum in the target chamber, large electromagnetic pulses, debris, plasma and hot electrons pose threat to electronic detectors

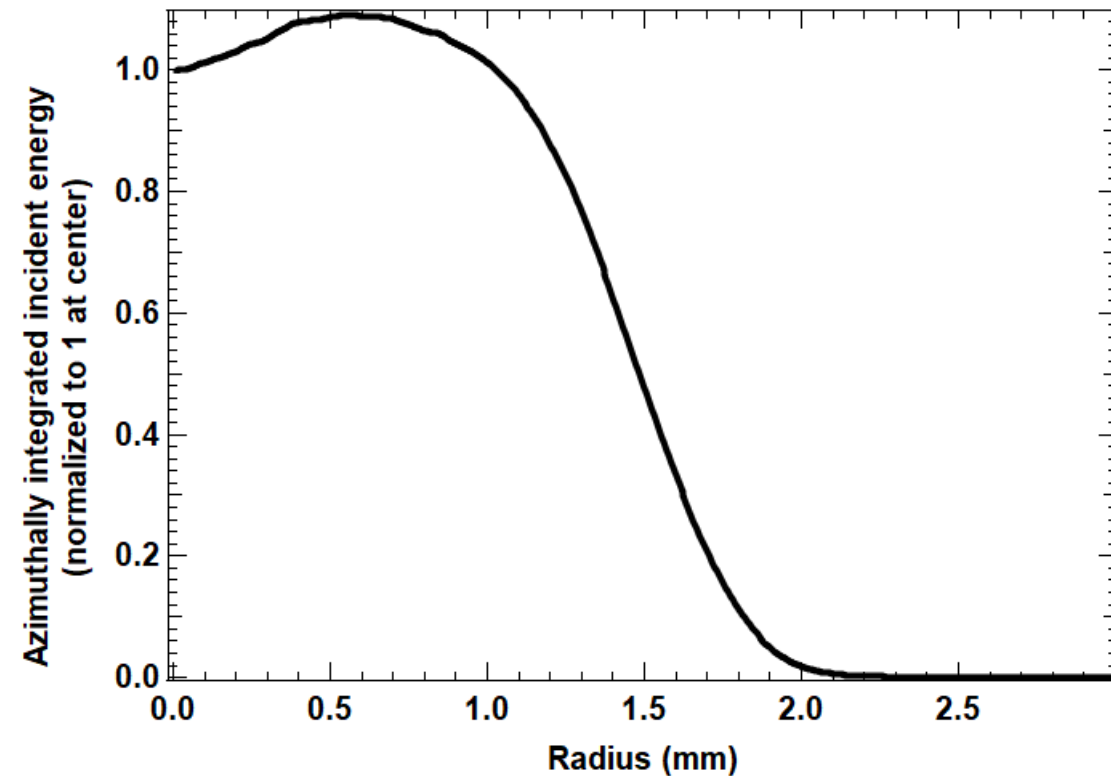


A shot time photograph (STP) image of the NIF target chamber

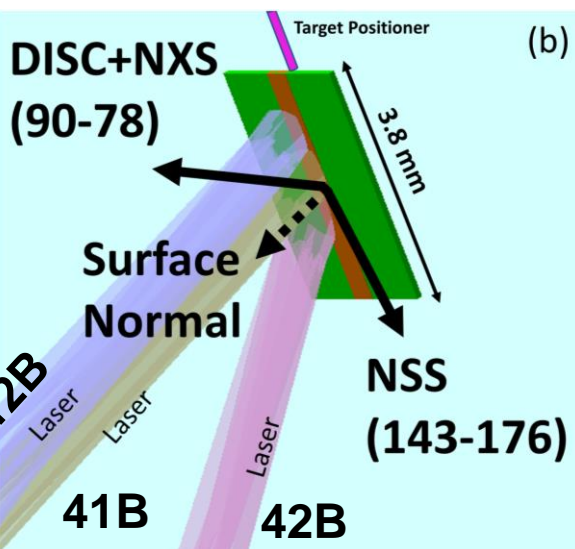
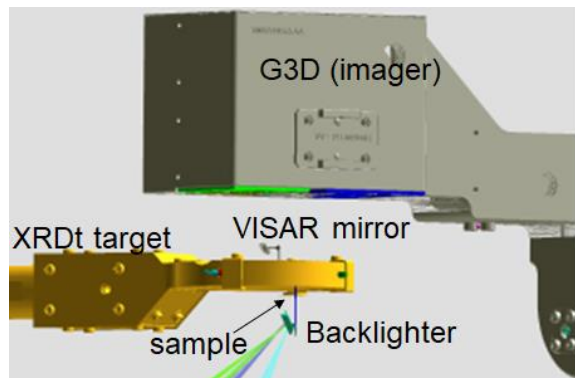
The drive laser transmits a compression wave into the sample while the pinhole collimates the x-rays towards the detectors



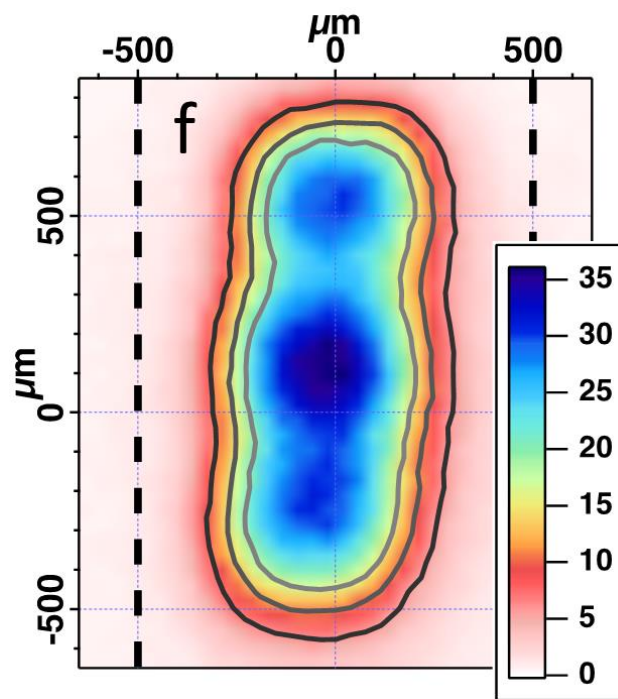
Predicted intensity variation for 14 beams pointed at the sample driven to Mbar pressures



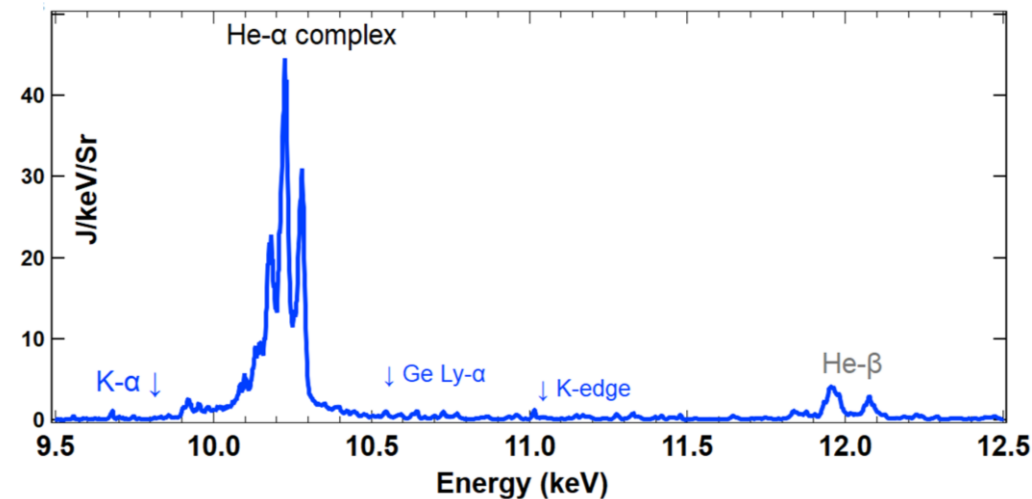
A germanium backlighter provides a nearly monochromatic x-ray source at 10 keV



X-ray emission footprint on the BL



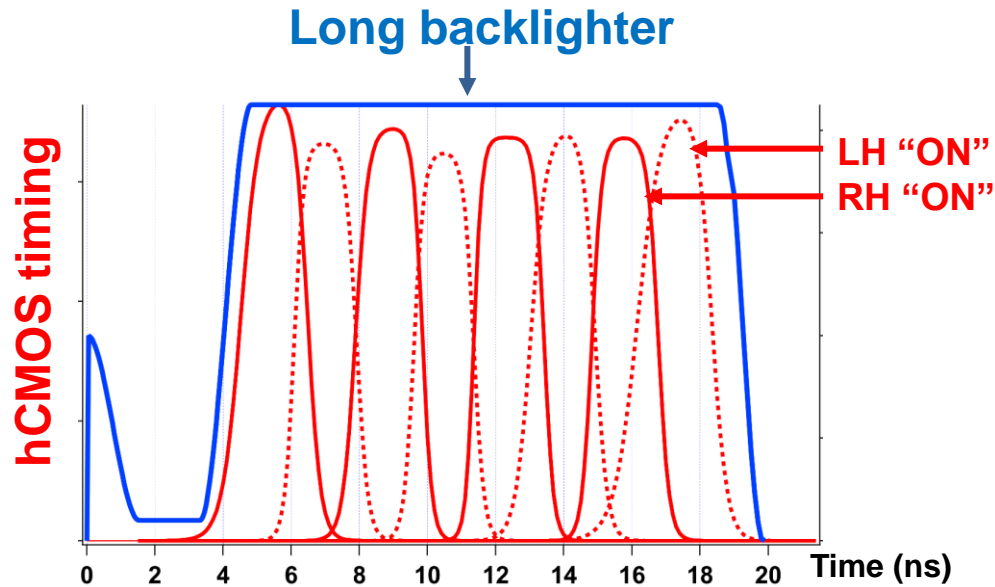
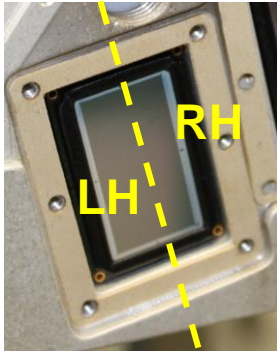
X-ray source spectrum



Werellapatha et al., RSI (2021)
Werellapatha et al., (submitted 2022)

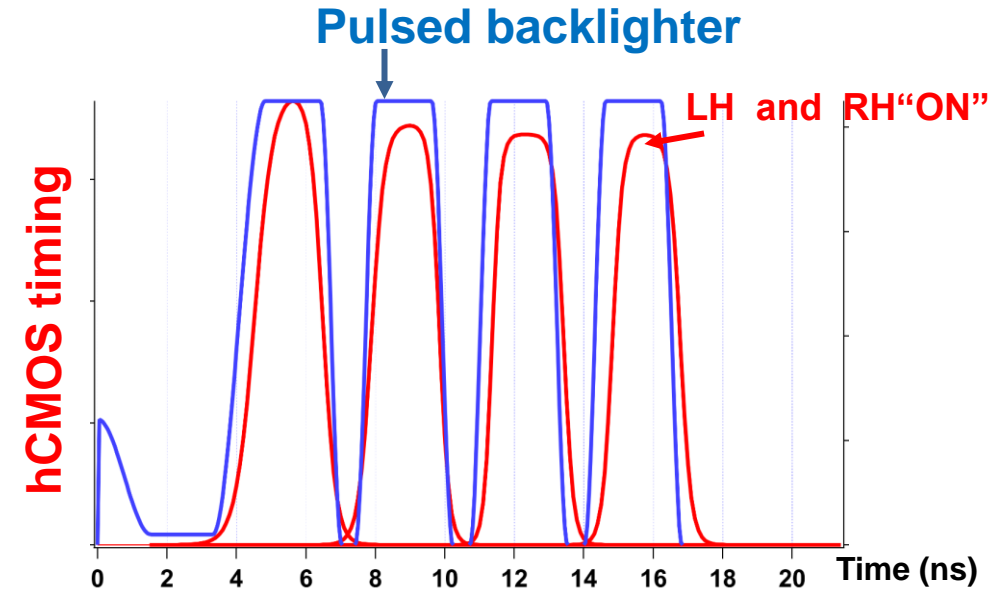
We designed two long duration BLs (~10ns) that match the operation of fast hCMOS sensors

Ultrafast hybrid-CMOS (hCMOS) Sensors (ICARUS sensors)



Continuous x-ray source for the entire hCMOS record when the two hemispheres are delayed in time

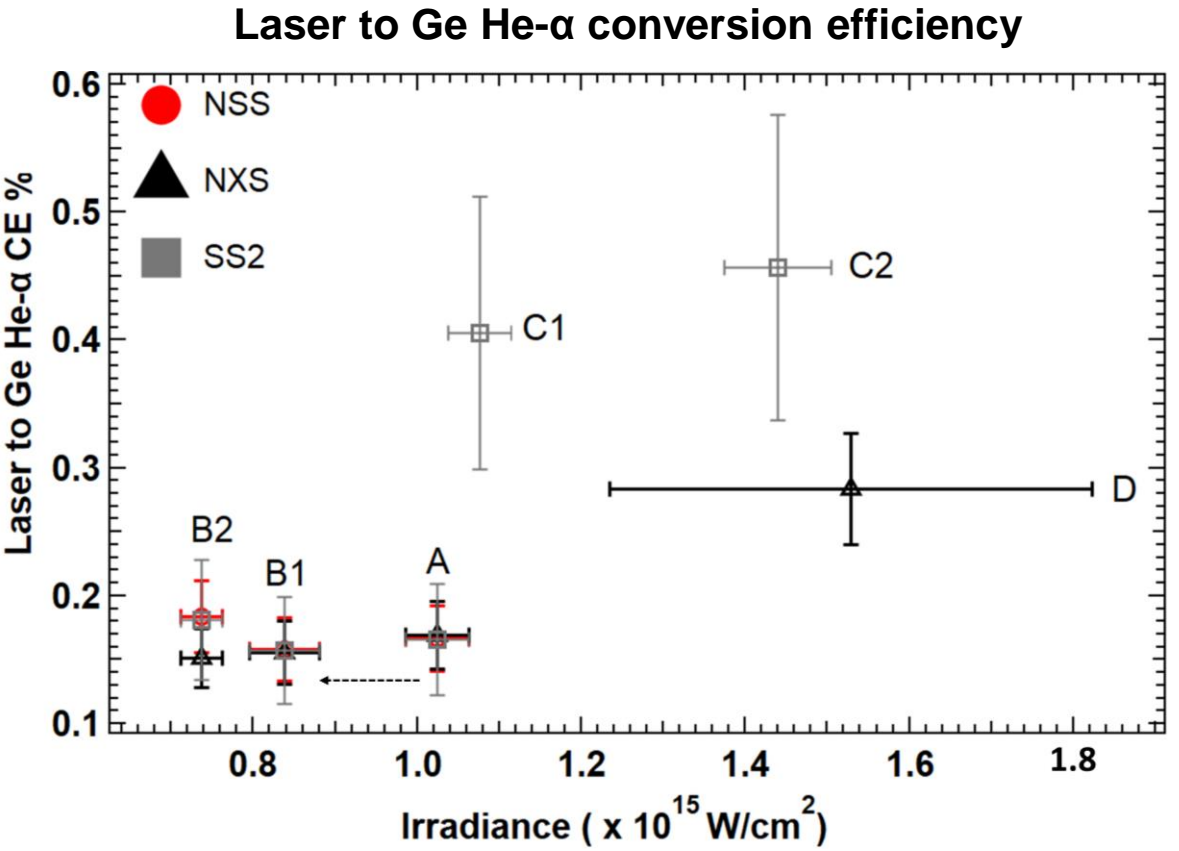
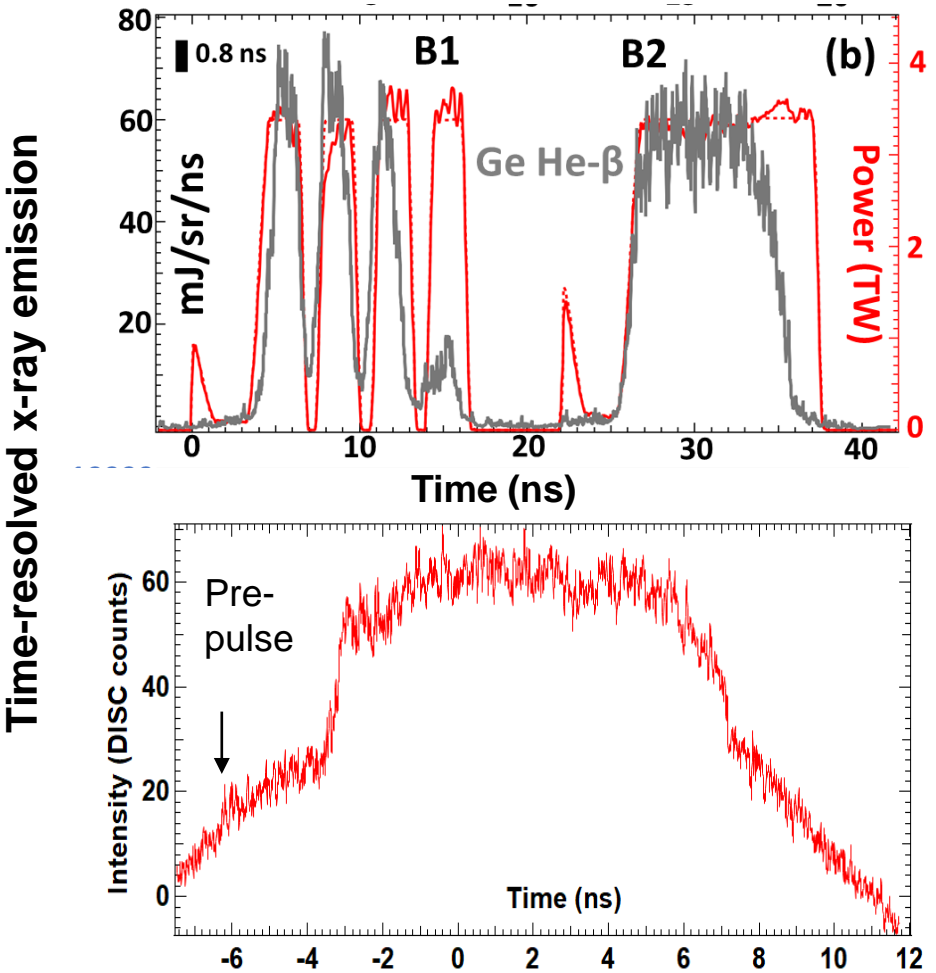
- Less angular coverage for XRD data
- + More temporal coverage



Pulsed x-ray source when both halves of the hCMOS are ON at the same time

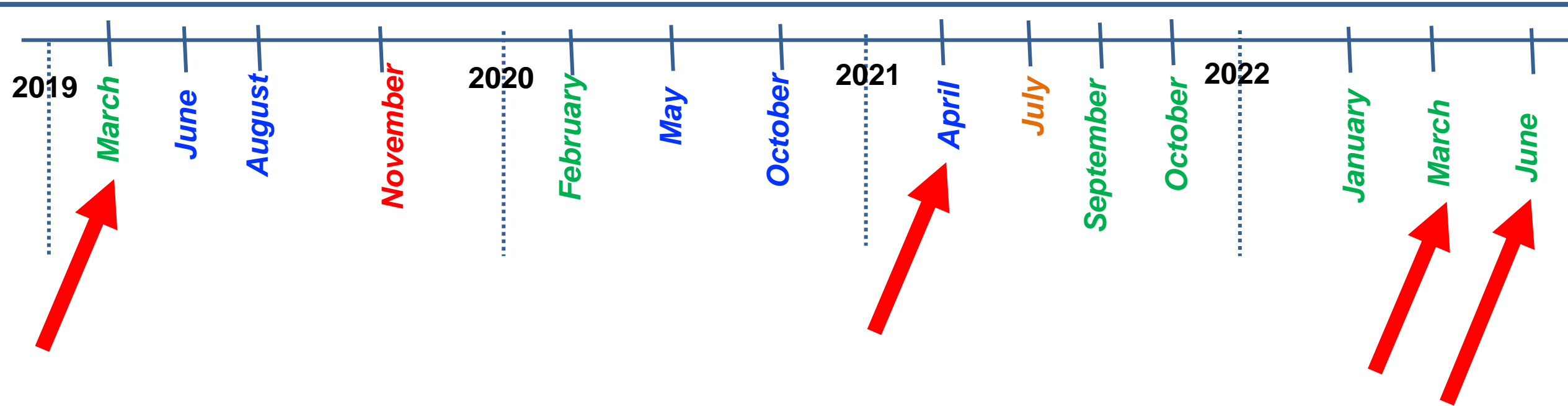
- + More angular coverage for XRD data
- Less temporal coverage

Our backlighter is either continuous or pulsed with a laser to x-ray conversion efficiency of ~0.5%



Werellapatha et al., (submitted 2022)

XRDt test diagnostic development involved a series of experiments at NIF



Capturing phase transition kinetics of Pb at 1 Mbar

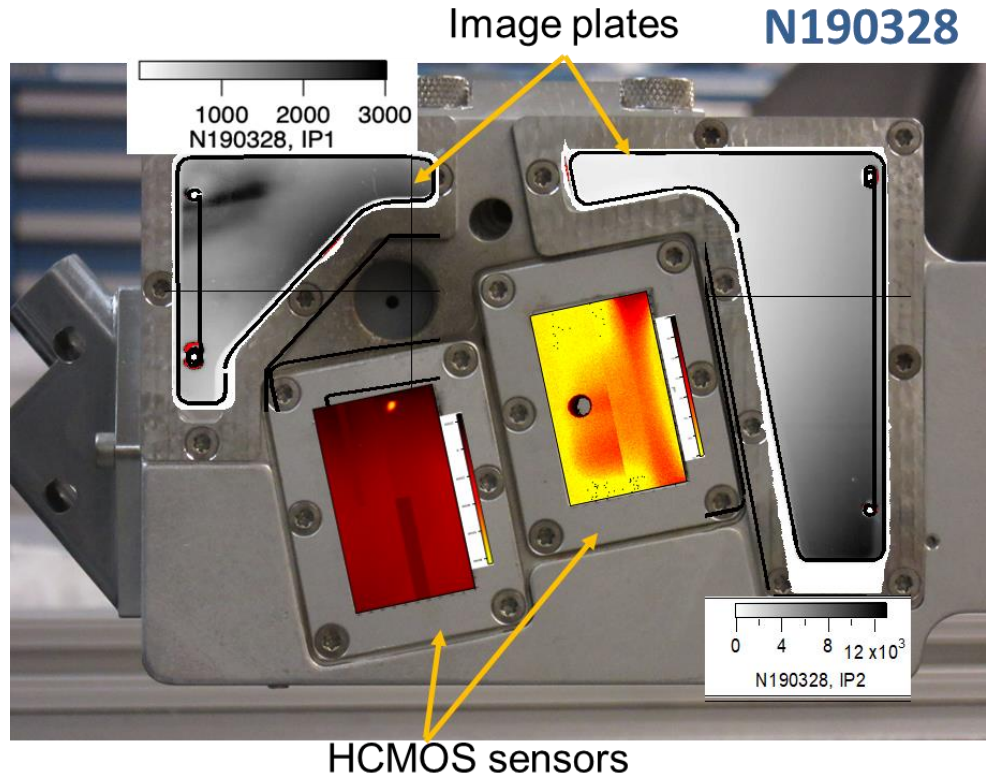
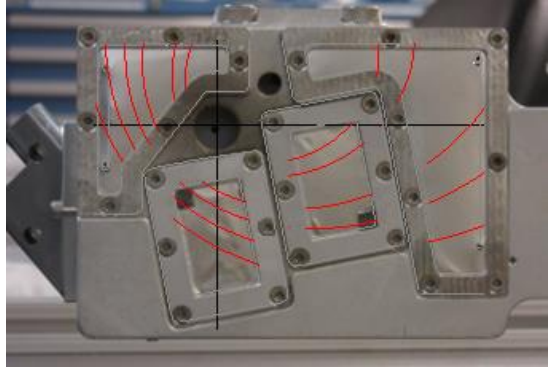
Drive laser background check at 200 GPa (drive lasers only)

Background mitigation at 0 GPa (backlighter only)

Understanding debris at 1000 GPa

We did not observe XRD in our initial shot due to high x-ray background, likely from hot electrons and x-ray fluorescence

N190328



No diffraction !

Background level approx. 10 times the XRD intensity on hcmos and IPs

The sensors were never damaged during the shot

Hypothesis:

Hot electron generation from the backlighter and x-ray fluorescence generation from target components produce the x-ray background

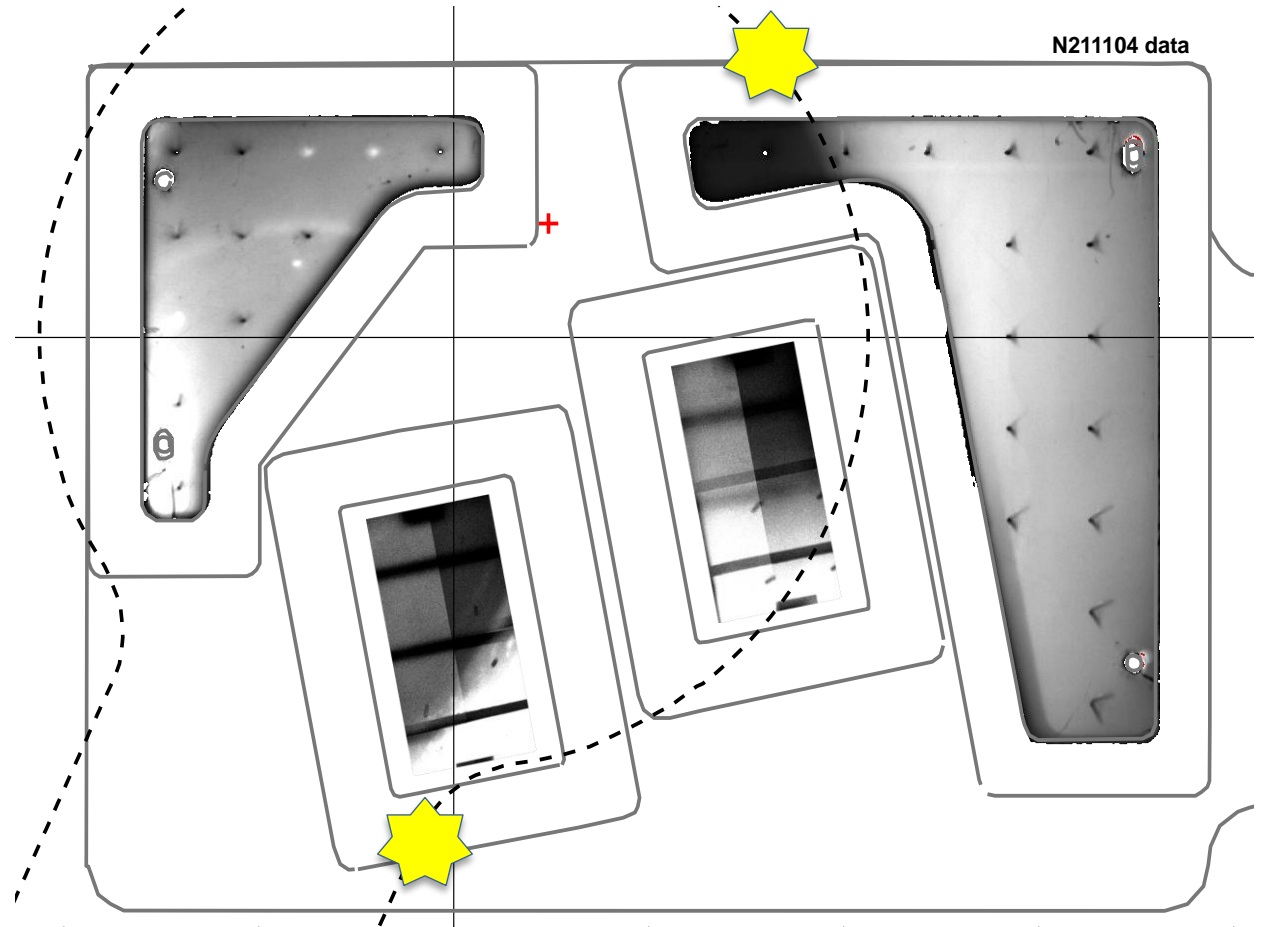
Background sources were traced using tungsten metal sentries attached to the sensors and image plates



Sentries on the sensors

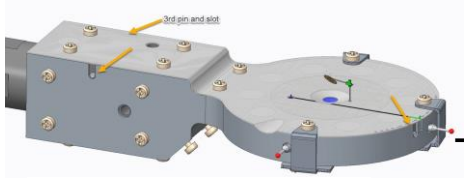
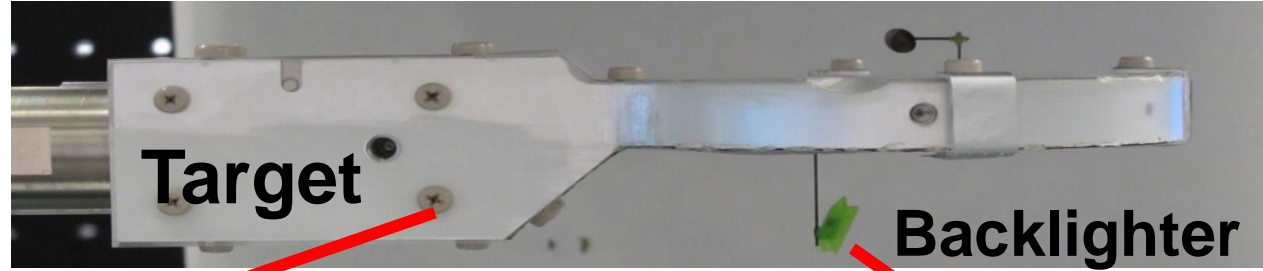
* Long shadows indicate source is at oblique angle to detector

* Short shadows indicate background source is more normal to detector surface



With multiple shadows we can ray trace to triangulate source location

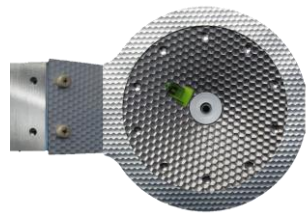
Heavy shielding needed either around the target or around the backlighter to mitigate background signal on the detectors



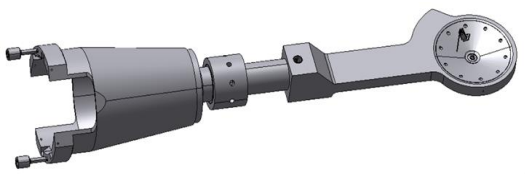
Top, bottom and sides shielded with various materials as a
-hot electron shield
 (with polystyrene, plastic)
-x-ray fluorescence shield
 (with Aluminum)



-Unconverted light dimples
 (on a bottom Al layer and later on, Ta target)



-Long-neck target



N200201

No shield around BL



N210407

300 μm microfine green plastic shield



N210422

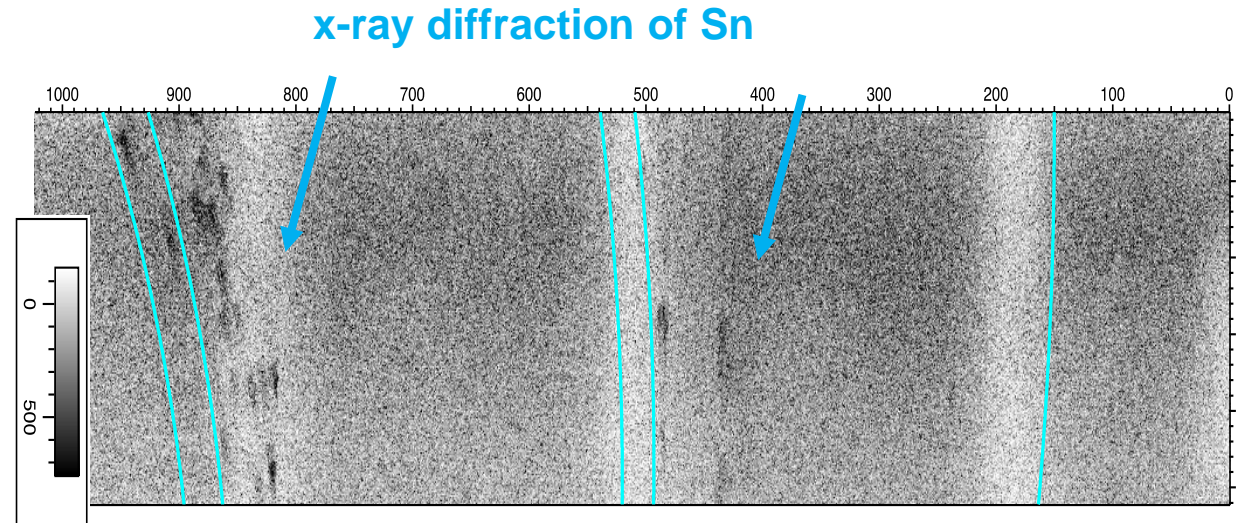
coated with 50 μm Au between plastic layers



N220310

roof extension coated with Au and plastic

We can observe x-ray diffraction and reduce background with shielding

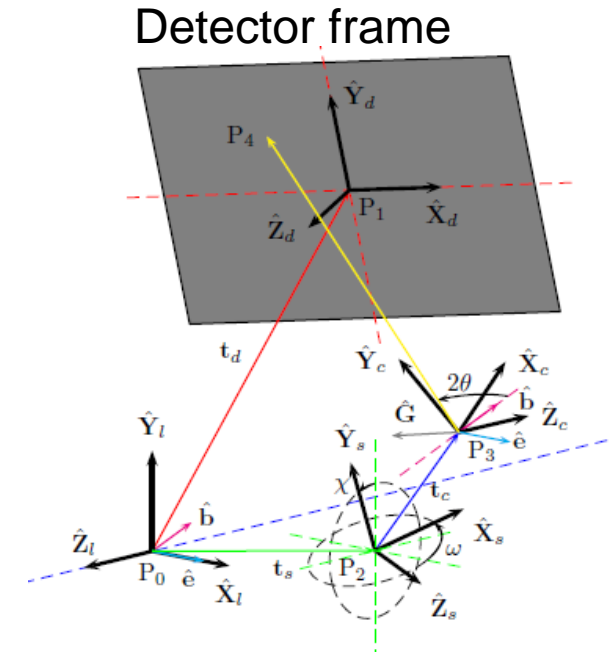
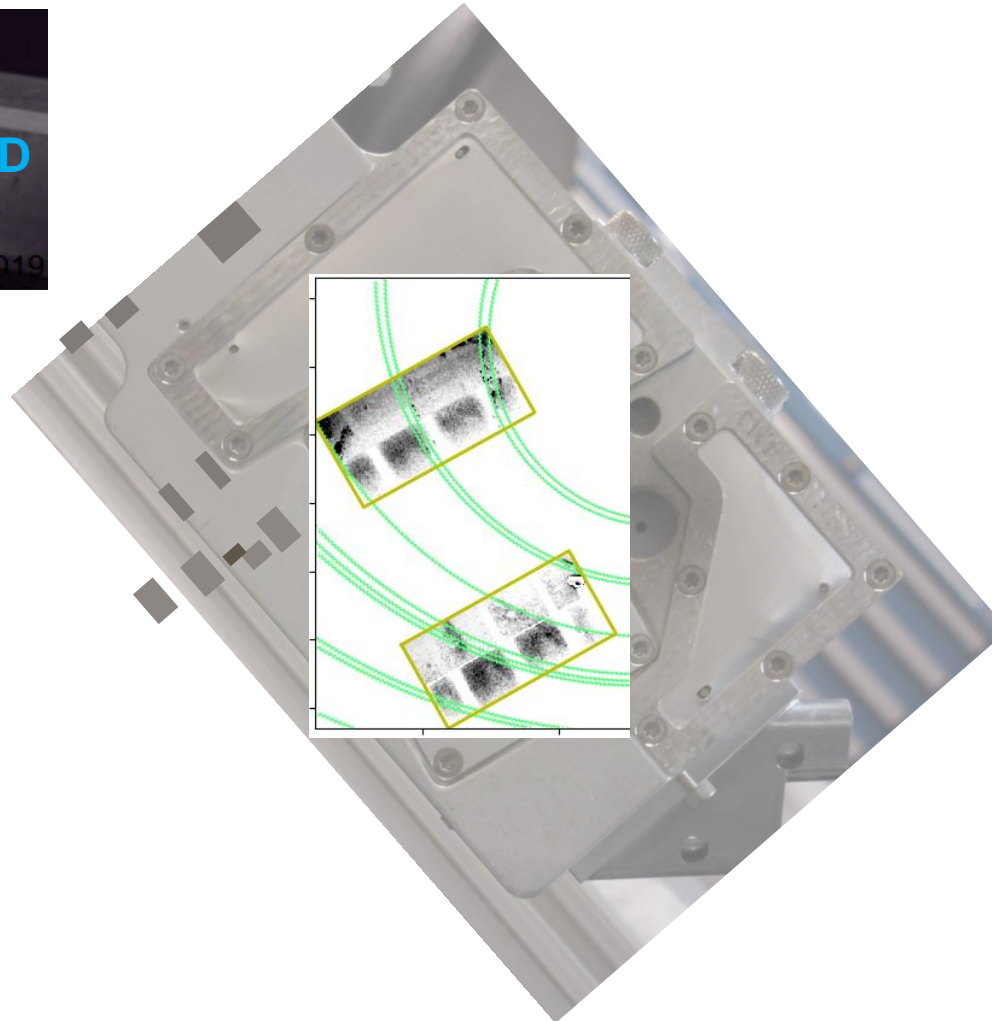
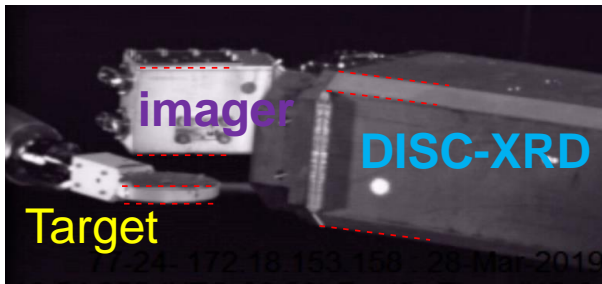


Credits: L.R Benedetti

The use of backlighter shield with plastic and Au was sufficient to give a ~10x reduction in x-ray background on our hCMOS detectors and it is the most effective method.

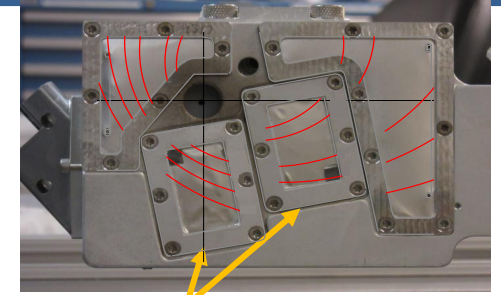
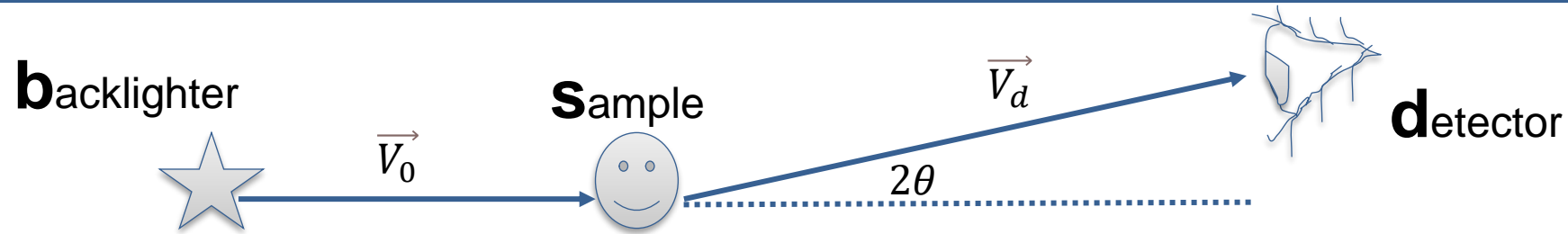
The undriven β -Sn shot was used to determine the location of the detector frame w.r.t the target in the NIF chamber

N210422



We use undriven β -Sn XRD to calibrate the translation and the tilt of the detector frame w.r.t the target in the NIF chamber

Any location uncertainty in the backlighter, sample and detectors in the NIF chamber result in location uncertainties in 2θ on the detectors



2 hCMOS sensors

Nominal scattering angle : $\cos 2\theta = \vec{V}_0 \cdot \vec{V}_d$; $\vec{V}_0 = (x_s - x_b)\hat{x} + (y_s - y_b)\hat{y} + (z_s - z_b)\hat{z}$
 ; $\vec{V}_d = (x_d - x_s)\hat{x} + (y_d - y_s)\hat{y} + (z_d - z_s)\hat{z}$

Uncertainty in nominal scattering angle on the detectors:

$$\delta(2\theta) = \pm \sqrt{\sum_i \left(\frac{\partial(2\theta)}{\partial x_i}\right)^2 \cdot (\delta x_i)^2 + \left(\frac{\partial(2\theta)}{\partial y_i}\right)^2 \cdot (\delta y_i)^2 + \left(\frac{\partial(2\theta)}{\partial z_i}\right)^2 \cdot (\delta z_i)^2}$$

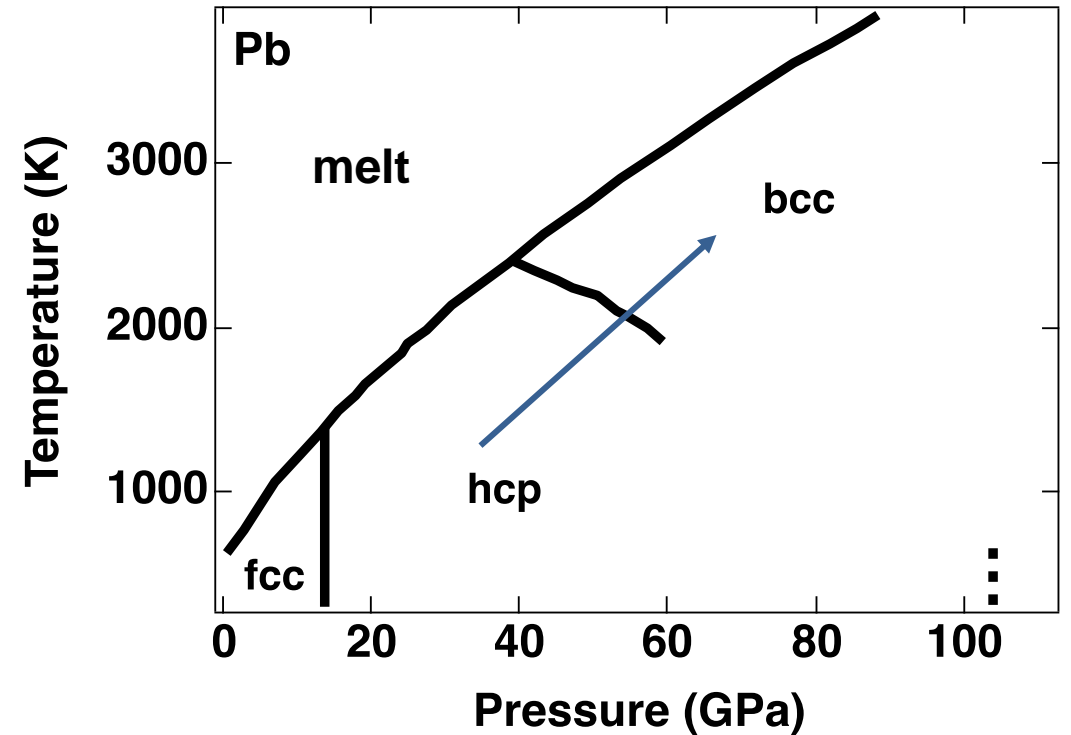
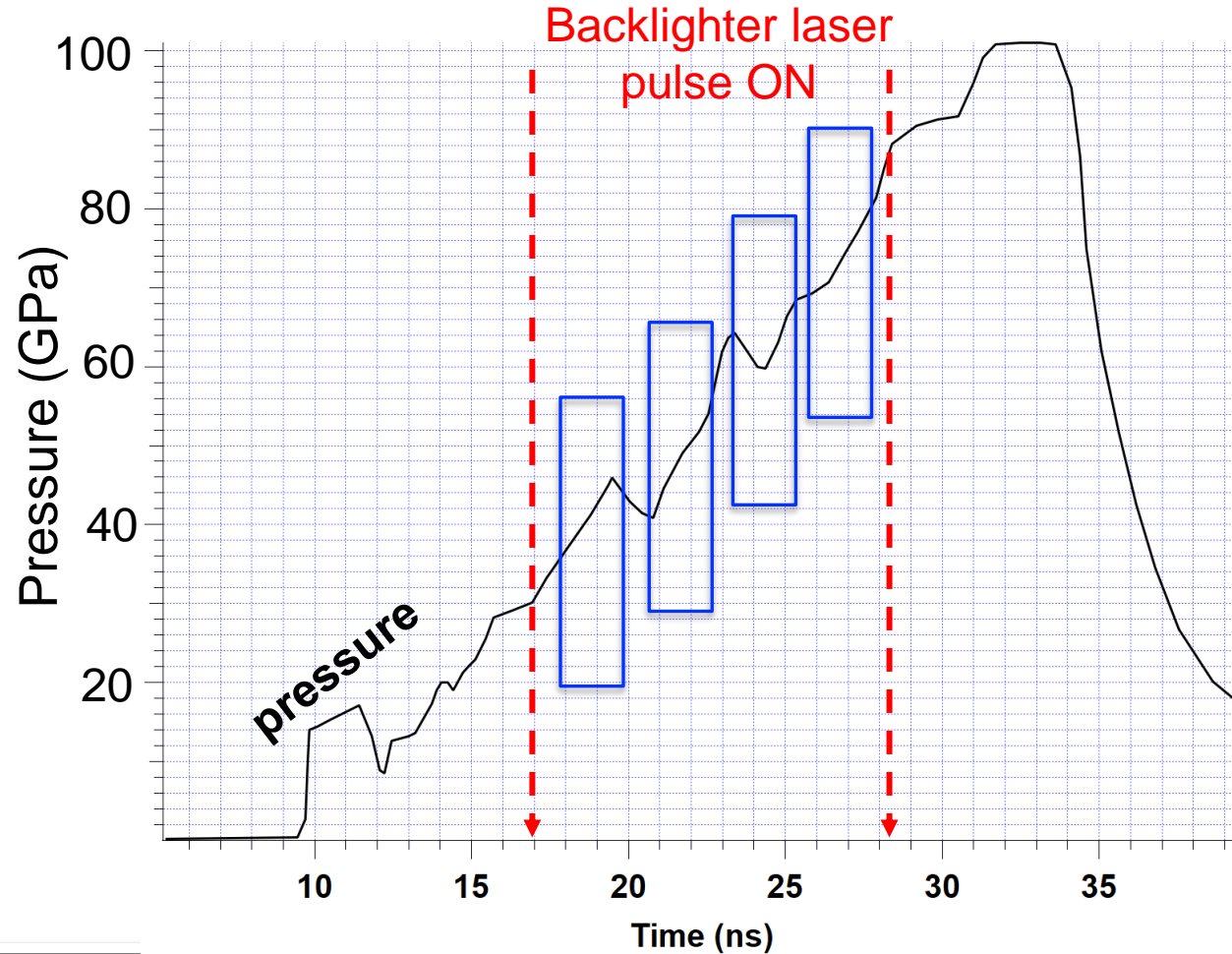
$i = b, s, d$

Preliminary calculations indicate an uncertainty range of 0.04° to 1.4° in 2θ across detectors due to location uncertainties in backlighter, sample and detectors in the NIF chamber

Preliminary calculations: K Werellapatha

We time the drive and the backlighter laser pulses to collect XRD data of dynamically compressed Pb during phase transitions

Typical timing diagram



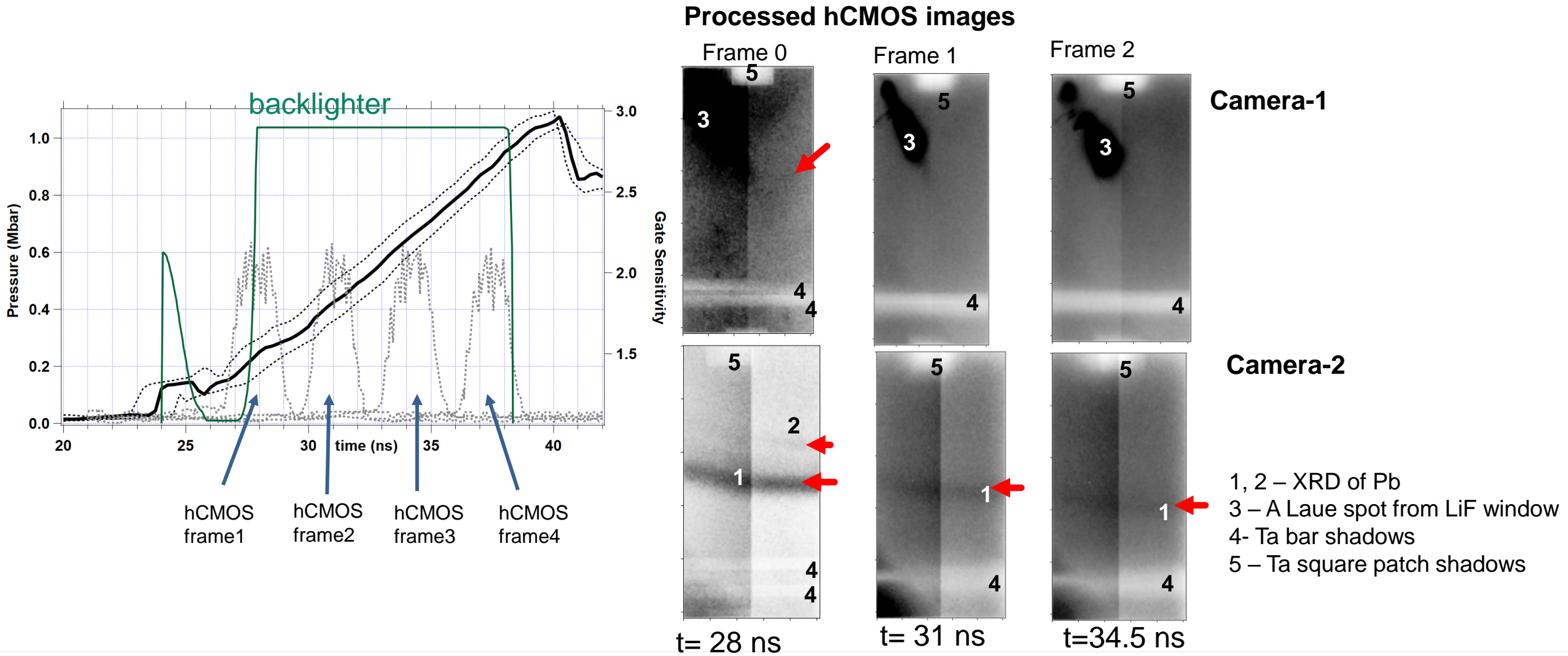
Multiple frames of hCMOS sensors captured driven Pb XRD data during two experiments with different parameters

Driven shots with good diffraction

	BL	BL energy	BL shield	Target bottom	Target neck	Phase transition observed
N220310	Zn	8.9 keV	Au, plastic, with roof	Dimpled Ta target body	Short	HCP to BCC (poor data quality)
N220621	Ge	10.225 keV	Au, plastic, with roof	Dimpled Ta target body	Long	HCP to BCC

X-ray diffraction data of Pb ramp compressed to 1 Mbar was captured by multiple frames of hCMOS sensors with a Zn backlighter

N220310

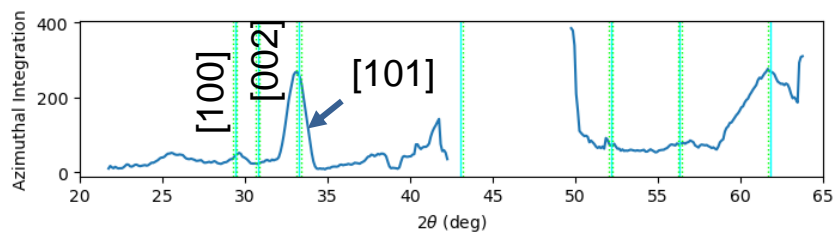
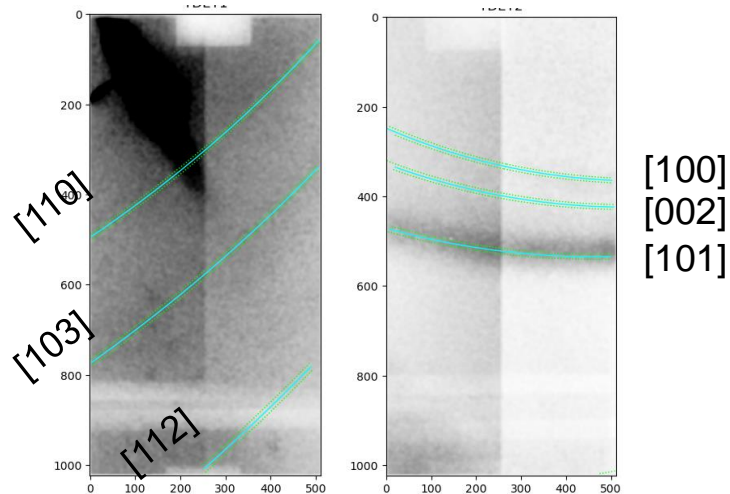


We observed Pb transforms from pure HCP to pure BCC at ~65 GPa within ~6.5 ns

N220310

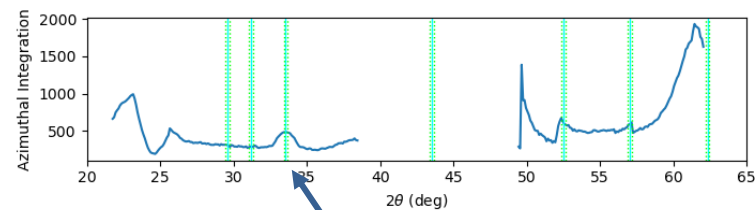
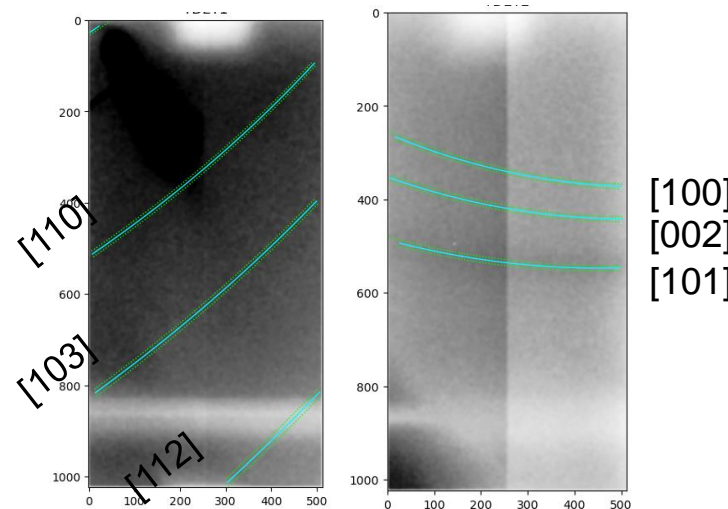
HCP Pb at ~25 GPa

$a = \sim 3.17 \text{ \AA}$
 $c = \sim 5.25 \text{ \AA}$
 $c/a = 1.66$



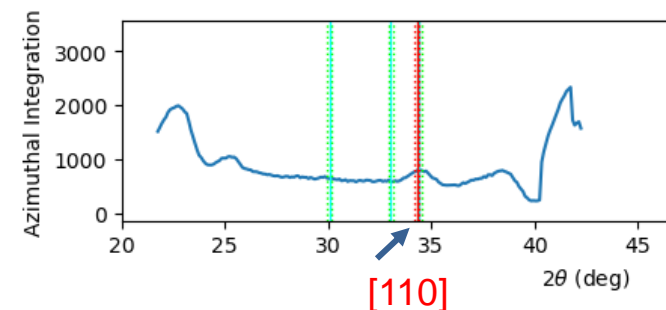
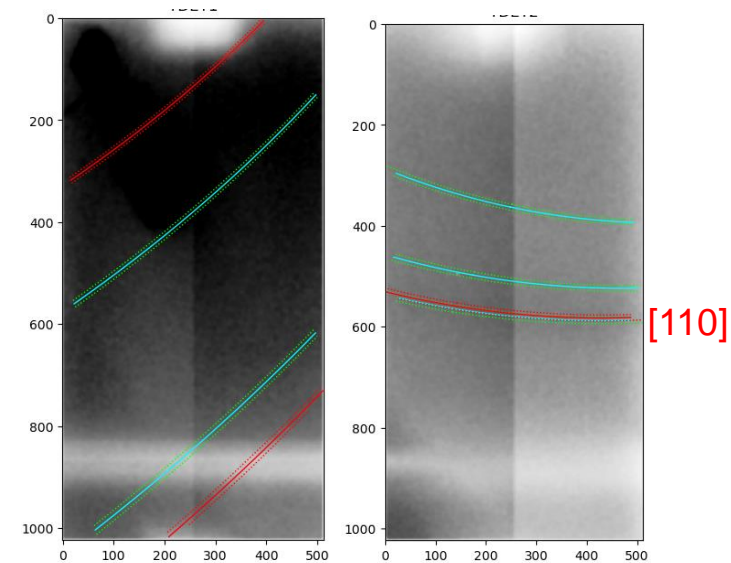
HCP Pb at ~30 GPa

$a = \sim 3.15 \text{ \AA}$
 $c = \sim 5.18 \text{ \AA}$
 $c/a = 1.64$



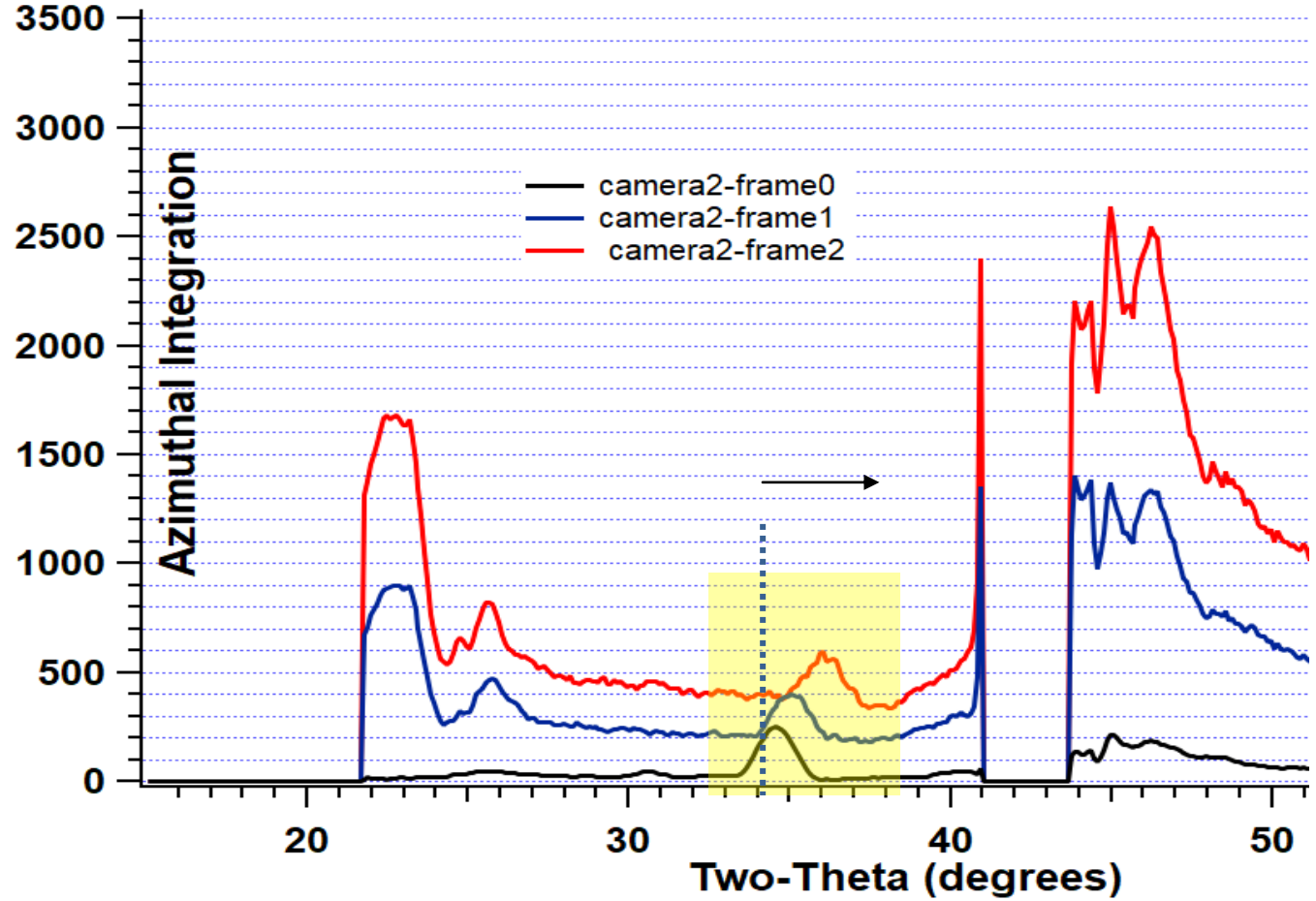
BCC Pb at ~65 GPa

$a = \sim 3.34 \text{ \AA}$



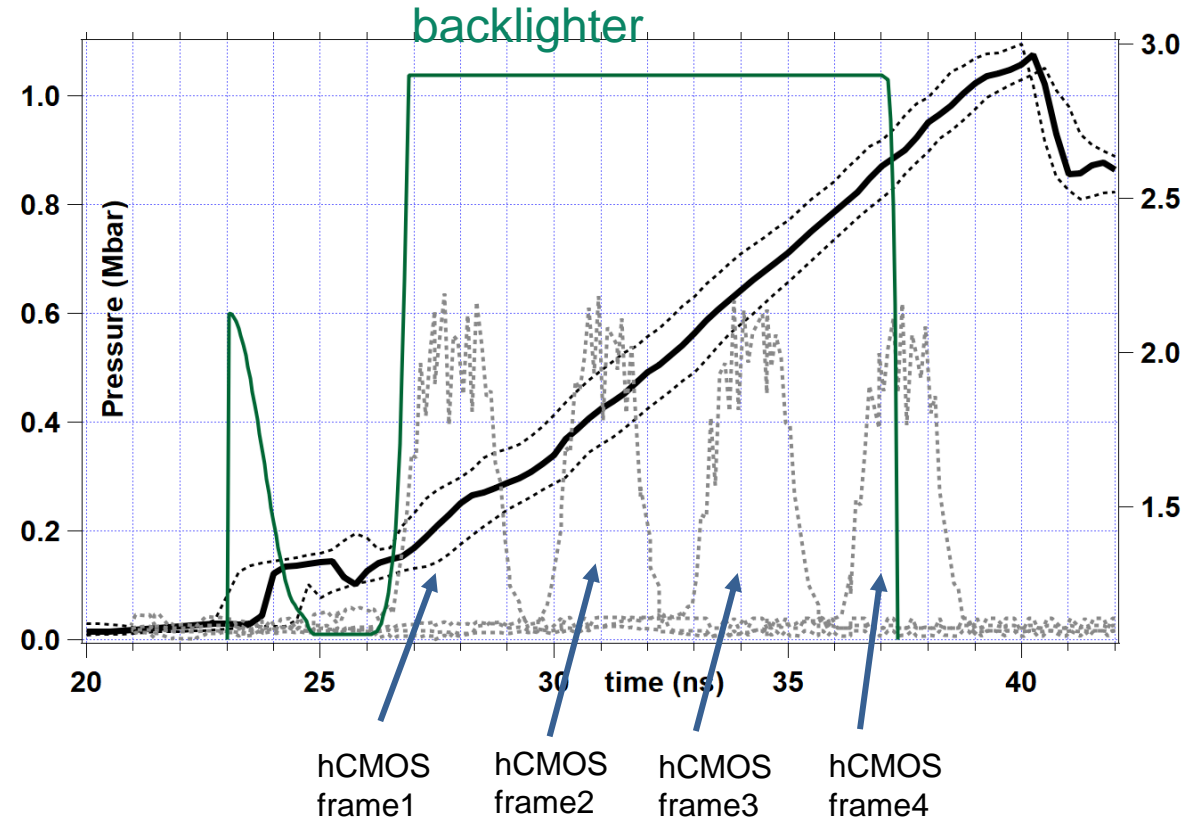
Preliminary diffraction analysis: K Werellapatha

The highest intensity XRD signal of HCP Pb moves to higher scattering angles as we increase pressure with time

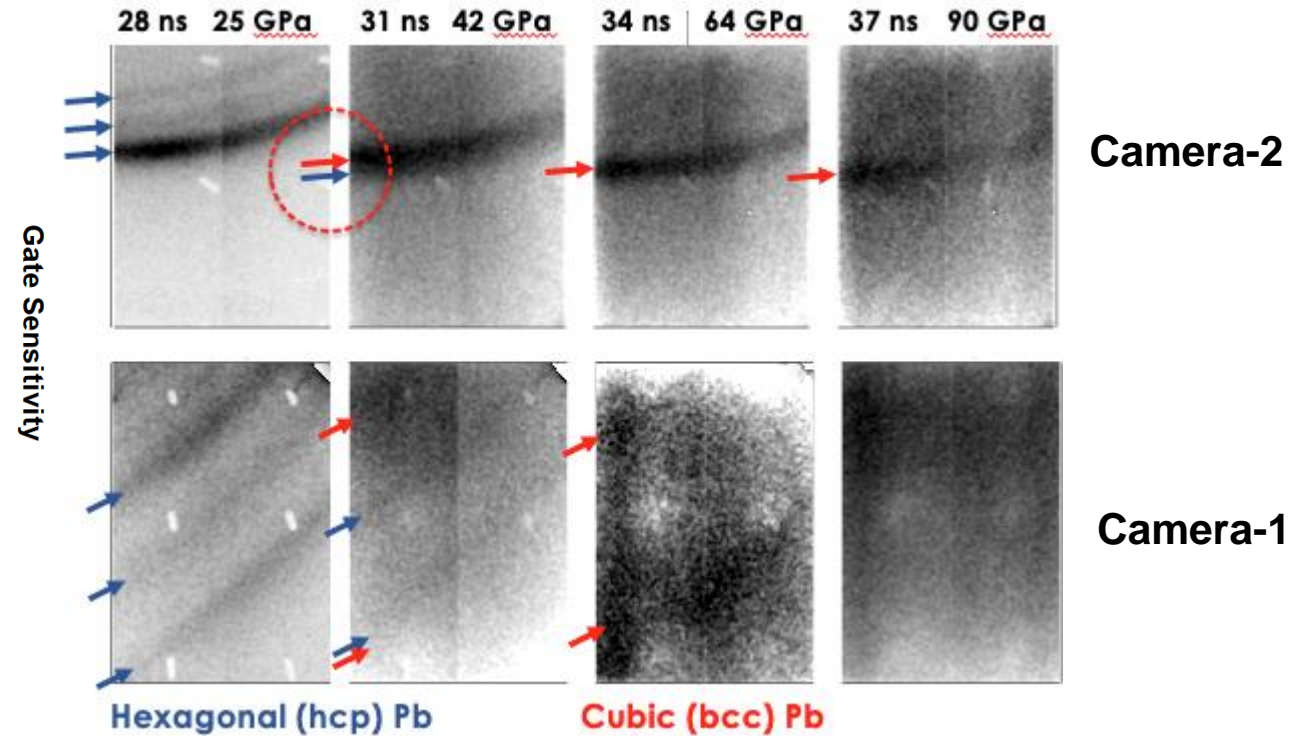


X-ray diffraction data of Pb ramp compressed to 1 Mbar was captured by multiple frames of hCMOS sensors with a Ge backlighter

N220621



Processed hCMOS images



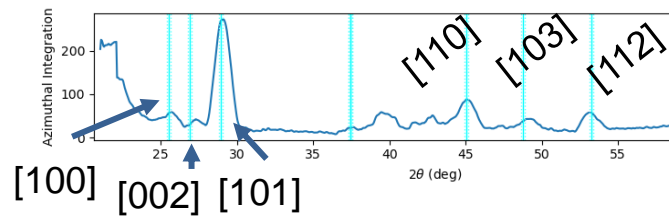
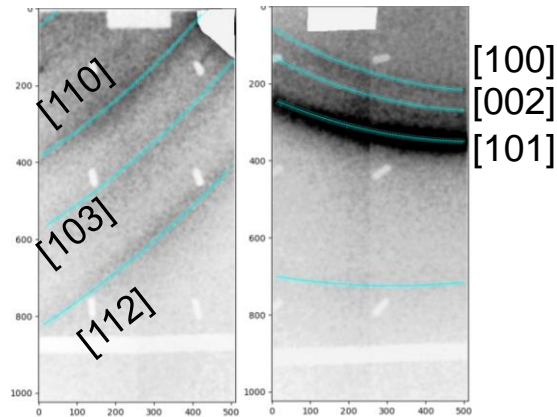
Credits: L.R Benedetti

We observed Pb transforms from pure HCP to pure BCC at ~65 GPa within ~6 ns

N220621

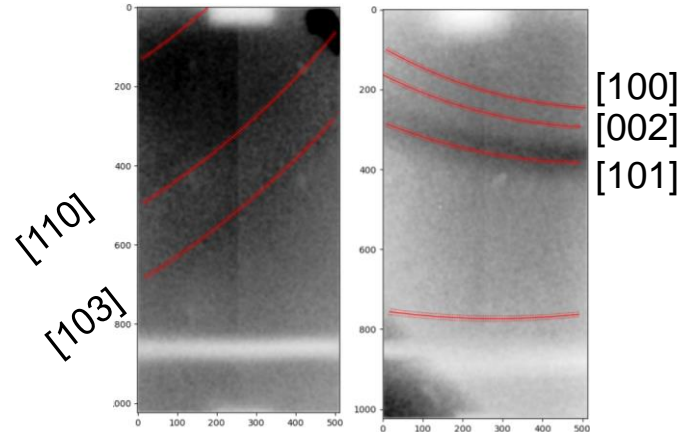
HCP Pb at ~25 GPa, 28 ns

$a = \sim 3.16 \text{ \AA}$
 $c = \sim 5.21 \text{ \AA}$
 $c/a = \sim 1.64$

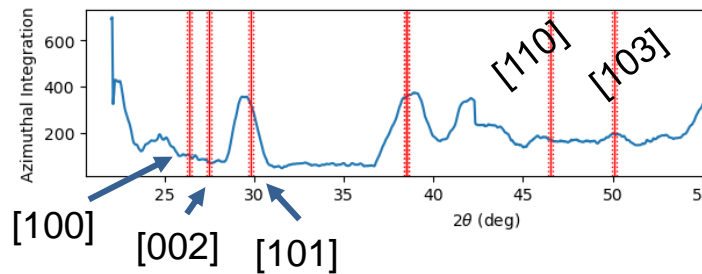


HCP Pb at ~40 GPa, 31 ns

$a = \sim 3.08 \text{ \AA}$
 $c = \sim 5.1 \text{ \AA}$
 $c/a = \sim 1.65$

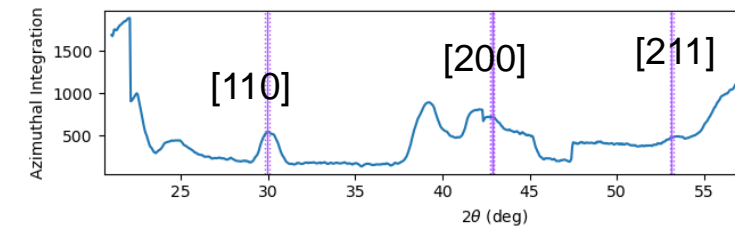
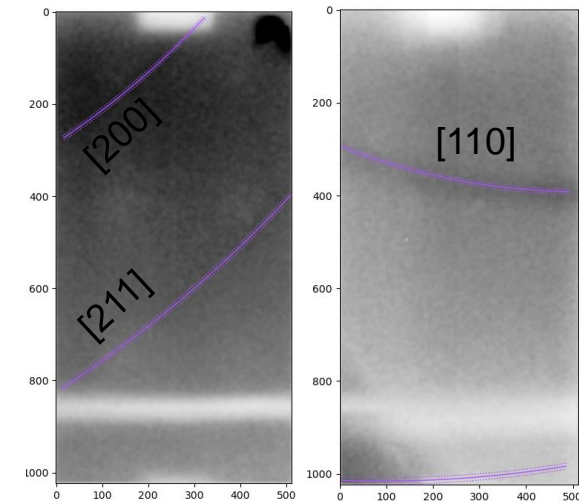


Line shape is consistent with a mixed phase



BCC Pb at ~65 GPa, 34 ns

$a = \sim 3.32 \text{ \AA}$



Preliminary diffraction analysis: K Werellapatha

We've developed a test diagnostic for time-resolved x-ray diffraction at the National Ignition Facility and are beginning to get good data

- Two hCMOS sensors with 1-2 ns exposure time can collect 4 frames of data during phase transition of Pb, ramp compressed to 1 Mbar
- We observed phase transition of Pb from HCP to BCC ~ 65 GPa within ~ 6 ns on a single shot
- We designed and optimized a ~ 10 ns long Ge backlighter as the x-ray source
- The design and development of this diagnostic will improve future XRDt diagnostics at the National Ignition Facility

Thanks



LLNL-PRES-837557

Prepared by LLNL under Contract DE-AC52-07NA27344

This document was prepared as an account of work sponsored by an agency of the United States government. Neither the United States government nor Lawrence Livermore National Security, LLC, nor any of their employees makes any warranty, expressed or implied, or assumes any legal liability or responsibility for the accuracy, completeness, or usefulness of any information, apparatus, product, or process disclosed, or represents that its use would not infringe privately owned rights. Reference herein to any specific commercial product, process, or service by trade name, trademark, manufacturer, or otherwise does not necessarily constitute or imply its endorsement, recommendation, or favoring by the United States government or Lawrence Livermore National Security, LLC. The views and opinions of authors expressed herein do not necessarily state or reflect those of the United States government or Lawrence Livermore National Security, LLC, and shall not be used for advertising or product endorsement purposes.

